Investigating accuracies of WorldView-2, Sentinel-2, and SPOT-6 in discriminating morphologically similar savanna woody plant species during a dry season

Emmanuel Fundisi,[a,]* **Solomon G. Tesfamichael,[a,]*** **and Fethi Ahmed[b]**

[a]University of Johannesburg, Department of Geography, Environmental Management and Energy Studies, Johannesburg, South Africa

[b]University of the Witwatersrand, School of Geography, Archaeology and Environmental Studies, Johannesburg, South Africa

Abstract. Accurate assessment of woody species diversity using remote sensing can assist ecologists by providing timely information for ecosystem management. The increasing availability of remotely sensed data necessitates the investigation of accuracies of different sensors in classifying plant species, especially during the dry season when foliage amount is low. WorldView-2, SPOT-6, and Sentinel-2 images were compared in detecting woody species ($n = 27$) and three coexisting land cover types in a savanna environment during a dry period. Random Forest (RF) and Support Vector Machine (SVM) classifiers were applied to each imagery to make a strong case for the comparison. The overall classification accuracies ranged between 52% and 65% for all images, with the WorldView-2 image performing the best followed by Sentinel-2 and SPOT-6 images. These accuracy rankings were similar for both the RF and SVM classifiers, with the former faring better. Pairwise comparison of the images using McNemar's test showed significant differences between images in their ability to correctly identify woody species. Analysis of band importance revealed better contributions to the classifications of infrared bands for all images. Overall, the findings showed the potential of optical imagery in classifying and monitoring woody species hotspots in savanna environments even during a low photosynthesis season. © 2022 Society of Photo-Optical Instrumentation Engineers (SPIE) [DOI: 10.1117/1.JRS.16.034524]

1 Introduction

Savannas occupy ∼20% of the entire Earth's surface, with 50% coverage of the African continent and 46% within the Southern Africa region.[1] Savannas also offer vital services to humans and the environment, such as the provision of grazing and browsing lands for livestock,[2,3] serving as a source of food and energy to humans,[4] and providing a natural habitat for wildlife.[5–7] Nonetheless, climate change and anthropogenic activities are threatening the savanna ecosystem through changes in weather patterns.[8] Furthermore, an uncontrolled increase in woody plants (woody encroachment) at the expense of other herbaceous plant species is also contributing to the imbalance of the savanna ecosystem.[9,10] Therefore, it is important to monitor savanna ecosystems in real time to manage these ecosystems efficiently.[11] Traditional approaches of quantifying woody plants through field surveys are expensive and can be subjective to the enumerator's interpretations, marred with unreliability and precision concerns.[12,13]

Remote sensing techniques are used as an alternative to field enumeration because they provide a reliable and efficient characterization of woody plant species. Several studies have exploited multispectral remote sensing to differentiate woody and nonwoody vegetation forms in both managed (e.g., Refs. 14 to 17) and natural forests (e.g., Refs. 10 and 18) at relatively high accuracy levels due to significant differences in the structural and chemical composition of the

---

*Address all correspondence to Emmanuel Fundisi, fundisye@icloud.com; Solomon G. Tesfamichael, sgtesfamichael@uj.ac.za

two plant forms. Such capability has been extended to identify a specific species from an ensemble of plant species in the savanna environments (e.g., Refs. 19 to 23). Focusing on a targeted species is important to manage, for example, invasive species and endangered plants.[19,20,22,24] However, from a remote sensing viewpoint, the identification of a single species remains fairly simple due to the homogeneity of chemical properties in the species of interest compared with cohabiting species.[25]

Monitoring multiple species types is essential for biodiversity assessment aimed toward maintaining ecological services and ecosystem functioning.[12,26] Multispectral images have been applied to differentiate multiple species types in the mangrove,[27] subtropics,[28] temperate regions,[29] boreal forest,[30] and tropical rainforest[31] with high accuracies achieved in most cases (>75%). Similar applications have been conducted in heterogeneous savanna environments (e.g., Refs. 10, 20, and 32). Reference 33 classified multiple species ($n = 40$) using both nonpansharpened and pansharpened Quickbird multispectral image. The authors evaluated classification performance using the overall kappa coefficient and recorded accuracies ranging between 0.48 and 0.99. Reference 34 compared the efficacy of SPOT-5 and Landsat-5 to discriminate multiple species ($n = 22$) and reported rather low accuracies (<53%) for both images. A common cause of inaccuracy in the classification of vegetation is a mixed pixel phenomenon due to mismatch between the scale of imagery and the variability in target species.[35,36] Accordingly, the images with low spatial and spectral resolutions relative to high-species diversity conditions lead to a misrepresentation of the plant variability that potentially exists in a localized environment. Therefore, it is important to find the balance between the scale of remotely sensed data and the size of individual plant species by comparing images with different spatial and spectral characteristics to enable accurate mapping of plant species in such environments.

Furthermore, the majority of savanna plant species classifications have been conducted in wet periods when most plants are photosynthetically active (e.g., Refs. 20, 37, and 38). Prominent differences in the chemical and structural composition of plant leaves during these periods induce distinguishable spectral signatures allowing for effective discrimination among plant species types.[39] Weather variations between wet and dry periods alter vegetation leaf development and senescence, with dry season exhibiting low foliage that may suppress the distinguishing traits among plants.[40] However, ecological monitoring requires knowledge about vegetation in dry season for a successful assessment throughout the year. Clear skies in dry seasons provide the ideal scenario for high-quality optical remotely sensed data that can be used for vegetation characterization. This has been demonstrated in a number of studies.[38,41–43] One notable example by Ref. 44 compared multiple images (Landsat and SPOT-5, moderate resolution imaging spectroradiometer, and GeoEye-1) in the savanna environment. However, that study focused on fractional cover estimation (quantifying the proportion of photosynthetically active and nonactive vegetation), rather than plant species classification. There is a need to compare multiple remotely sensed data to classify morphologically similar woody plant species in dry seasons.

Therefore, this study aimed to investigate the performances of WorldView-2, SPOT-6, and Sentinel-2A images in detecting several woody plant species ($n = 27$) and coexisting land cover types (bareland, grassland, and shrubs) in a savanna environment during a dry season. These images have different spatial and spectral characteristics and therefore could provide an insight into the optimal data characteristics needed for monitoring woody species diversity in savanna environments. The study used an area with relatively high species diversity consisting of a mix of young and mature narrow-leaved woody plant species.

2 Methods

2.1 Study Area

The Klipriviersberg Nature Reserve (KNR) located in Johannesburg, South Africa, was used for the study (Fig. 1). The reserve was declared a nature conservation area in 1984 and covers ~651 ha. In general, the vegetation types in the reserve include Andesite Mountain Bushveld and Clay Grassland, which are associated with a savanna environment.[45] The altitude of the area
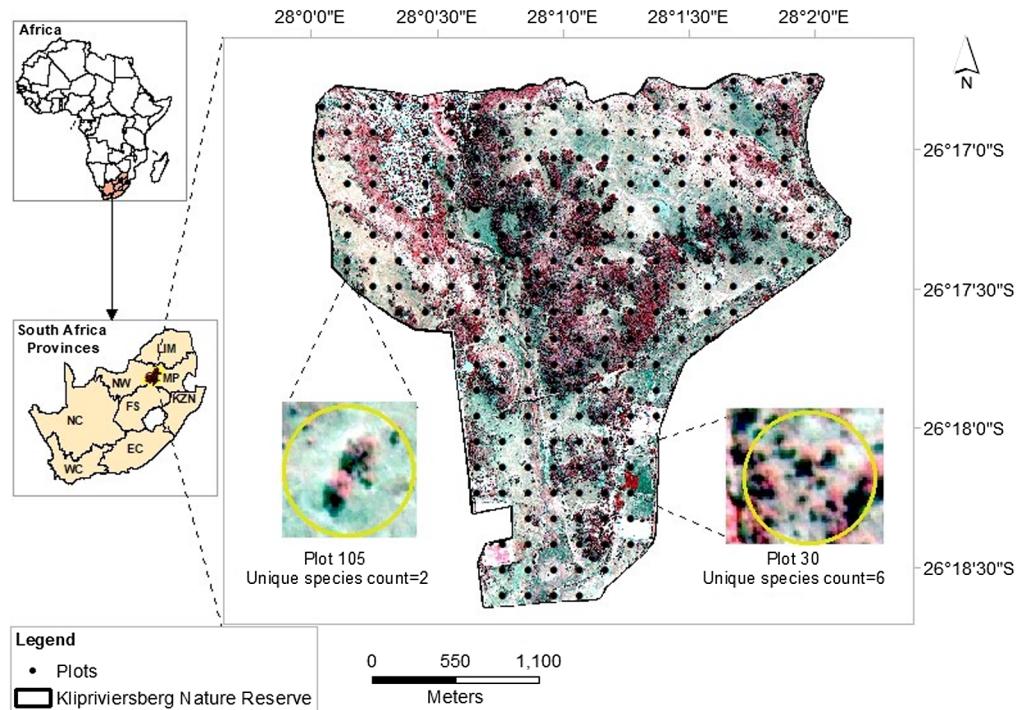
Fig. 1 Klipriviersberg Nature Reserve and the distribution of sampling plots used in the study. The background image was derived from a WorldView-2 image in false color composite (red, band 6; blue, band 4; green, band 5).

ranges between 1540 m in the south and 1790 m in the north, with a mean altitude of 1653 m. The mean annual rainfall around KNR ranges from 624 to 802 mm promoting foliage and canopy cover in wet periods. The wet season, which is largely associated with photosynthetically active plants, runs from November to March and the dry season associated with low foliage occurs between May and October. The mean annual temperature ranges between 17°C and 26°C in summer and 5°C and 7°C in winter.[46] The geology types found in the area, which lead to the floristic structure of the reserve, include quartzites, conglomerates, and dolomites.[47]

2.2 Field Data

In this study, 240 points distributed at ∼170 m intervals in the north–south and east–west directions were generated in ArcGIS (ESRI® ArcGIS 10.6, Redlands, California). The point coverage was exported into a global positioning system (Garmin, GPSMAP® 64, Kansas) and located in the field. Field surveys were conducted from May to June, 2017, representing the dry period in the study area.[46] A buffer with a 20-m radius was created around each point, making a plot; this size was specified to accommodate multiple pixels of the images used in the study (WorldView-2, SPOT-6, and Sentinel-2A). Circular plots were preferred over rectangular plots as they require only a single control point at the plot center.[48] Furthermore, circular plots were favored instead of angular shapes, since circular canopy shapes are more commonly witnessed in a natural vegetation environment. In each plot, plant species with height ≥2 m and land covers were recorded, with the record showing a minimum of one and a maximum of nine different species per plot. Overall, a total of 27 different species and three land cover types (grassland, bareland, and shrubs) were recorded in all plots. Additional structural attributes, such as species canopy size and species richness, were recorded in each plot. These attributes were used to confirm the assignment of a pixel to a class in an instance of mixed-pixel phenomenon. Accordingly, a pixel was allocated to species that had the dominant canopy size falling within that pixel. In the case of multiple plants with relatively small canopy sizes, the species with the most occurrence determined the classification of that pixel.

2.3 Remote Sensing Data and Preprocessing

WorldView-2, SPOT-6, and Sentinel-2A were acquired on May 17, June 5, and June 10, respectively, coinciding with the time of the field surveys. WorldView-2 image (DigitalGlobe)[49] has eight multispectral bands in the 0.40 to 1.04 μm region and a panchromatic band in the 0.45 to 0.80 μm (Fig. 2) measured at 1.8 and 0.46 m spatial resolutions, respectively. SPOT-6 image was sourced from the South African National Space Agency (SANSA). The imagery has four multispectral bands in the 0.45 to 0.89 μm and a panchromatic band in the 0.45 to 0.75 μm (Fig. 2) measured at 6 and 1.5 m spatial resolutions, respectively. Sentinel-2A image was downloaded from the European Space Agency Data Hub.[50] Sentinel-2 has 13 multispectral bands (Fig. 2) with four bands (0.49 to 0.84 μm) measured at 10 m spatial resolution and six bands measured at 20 m spatial resolutions. Prior to classification, the three images underwent atmospheric correction to ensure high signal-to-noise ratio. A comparison of atmospheric correction methods between dark object subtraction (DOS)[51] and fast line-of-sight atmospheric analysis of hypercubes[52] showed strong similarities between the two approaches (Pearson's correlation, $r = 0.95$). Therefore, we applied DOS to all individual bands of each imagery in ENVI 5.3 (©2015 Exelis Visual Information Solution Inc., Boulder, Colorado). Coastal bands were excluded due to the relative sensitivity of those bands to atmospheric interferences.[53] The remaining bands (7 for WorldView-2, 4 for SPOT-6, and 10 for Sentinel-2A, Table 1) were subsequently pansharpened. Notably this study utilized the Gram–Schmidt algorithm[54] which maximizes image sharpness and minimizes color distortions.

2.4 Training and Classification of Remotely Sensed Data

Training of 27 unique woody plant species as well as grassland, shrubs, and bareland classes was performed on the three satellite images (WorldView-2, SPOT-6, and Sentinel-2A) separately. It should be noted that as the spatial resolution becomes coarser, individual pixels are less likely to capture small features resulting in mixed pixel phenomenon.[39,55,56] This study adopted the nearest-neighbor resampling technique on SPOT-6 and Sentinel-2A to resample the pixels to the size of the WorldView-2 image (0.5 m). Nearest-neighbor resampling technique was chosen because it does not alter values in the output raster data set and therefore appropriate for categorical data classification.[57] Resampling to 0.5 m ensured exact subdivision of Sentinel-2A and SPOT-6 images avoiding the mixing of information between neighboring pixels of the original resolutions. By superimposing the three images, it was also confirmed that the offset in the pixel locations never exceeded 0.03 m avoiding the spill effect of information into neighboring pixels.
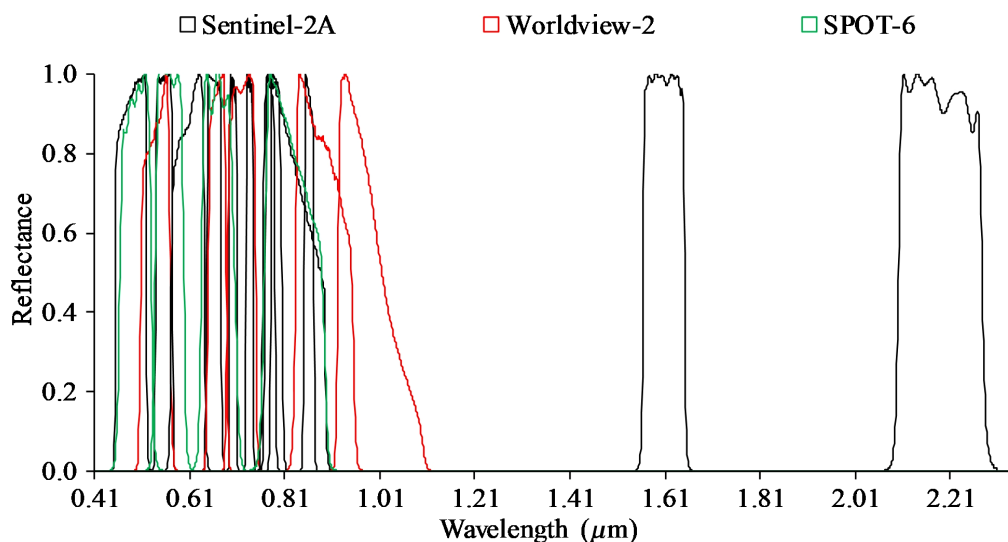
Fig. 2 Spectral profiles extracted from satellite images used in the study.

Table 1 Comparison of spectral and spatial profiles of satellite images used in the study.

Worldview-2			Sentinel-2A			SPOT-6		
Band name	Wavelength range (center wavelength) μm	Spatial resolution (m)	Band name	Wavelength range (center wavelength) μm	Spatial resolution (m)	Band name	Wavelength range (center wavelength) μm	Spatial resolution (m)
Panchromatic	0.45 to 0.80 (0.47)	0.5	—	—	—	Panchromatic	0.45 to 0.52 (0.47)	1.5
Blue	0.45 to 0.51 (0.48)	2	Blue	0.45 to 0.52 (0.49)	10	Blue	0.45 to 0.52 (0.48)	6
Green	0.51 to 0.58 (0.55)	2	Green	0.54 to 0.57 (0.56)	10	Green	0.53 to 0.59 (0.56)	6
Yellow	0.58 to 0.62 (0.61)	2	Red	0.65 to 0.68 (0.66)	10	Red	0.62 to 0.69 (0.71)	6
Red	0.63 to 0.69 (0.66)	2	Red edge 1	0.69 to 0.71 (0.70)	20	NIR	0.76 to 0.89 (0.80)	6
Red edge	0.70 to 0.74 (0.72)	2	Red edge 2	0.73 to 0.74 (0.74)	20	—	—	—
NIR-1	0.77 to 0.89 (0.83)	2	Red edge 3	0.77 to 0.79 (0.78)	20	—	—	—
NIR-2	0.86 to 1.04 (0.95)	2	NIR	0.78 to 0.90 (0.84)	10	—	—	—
	—	—	Narrow NIR	0.85 to 0.87 (0.86)	20	—	—	—
	—	—	Shortwave infrared-1	1.56 to 1.65 (1.61)	20	—	—	—
	—	—	Shortwave infrared-2	2.10 to 2.28 (2.20)	20	—	—	—

Similar sampling points were used for the three images to ensure direct comparability between results. A total of 8011 points representing 27 woody plant species, grassland, shrubs, and bareland were digitized inside the 240 plots on the three satellite images separately. Digitizing of points was guided by field surveys in which a local Cartesian coordinate system was used to locate the species. Finally, points were split into two portions of which 30% ($n = 2408$) were allocated to training–classification and 70% ($n = 5603$) to evaluate the accuracy of the classification. The spatial distribution of the training samples was taken into consideration when selecting the training samples. The species along with the proportions allocated to the training and testing of the classifications are given in Table 2.

Two machine learning classification algorithms utilized in this study are Random Forest (RF) and Support Vector Machine (SVM). These classification algorithms were implemented using the Caret package[58] for R language.[59] The RF classifier is an ensemble machine learning approach, which utilizes bootstrap sampling to build multiple decision tree models.[60] The RF method was selected for this study due to the following reasons: (i) it can analyze large datasets, (ii) it is free from normal distribution assumptions, and (iii) it is powerful when dealing with outliers in the dataset.[61] Internally, the RF uses two-thirds of the data (in-bag) for training the classification model and the remaining one-third, which is referred to as out-of-bag data, to evaluate the accuracy of the trained model.[61] RF classifier utilizes *ntrees* (number of classifications trees) and *mtry* (a number of predicting variables) to generate a prediction model.[60] In this study, a 10-fold cross-validation analysis which was repeated 10 times was used to determine the optimal parameters. The explanatory power of the input variables (multispectral bands) was quantified to rank the importance of each band for the classification accuracy.

The SVM approach classifies features (reflectance of different bands) by identifying optimal decision (separation) boundary that maximizes the margin between two classes.[62] The SVM, such as the RF, does not require the data to have a normal distribution,[63] and it performs well when using high dimensional and complex data. This study used a nonlinear SVM technique, i.e., radial basis function kernel that accommodates linear and nonlinear relationships between a response and a predictor[62] customized for R.[64] The SVM classifier requires the specification of two parameters to balance the accuracy and reliability of the classification.[63] These parameters include cost factor (C) and gamma (γ). The C factor relates to the penalty (cost) of misclassification error, and γ determines the influence of a training sample to capture the complexity in the data.[62] C and γ were also determined by running 10-fold cross-validation which was repeated 10 times similar to the approach applied for selecting optimal parameters of the RF. Training and classification of the images were performed on 30% ($n = 2408$) of the data using each satellite image.

2.5 Accuracy Assessment

Classification results derived from the remotely sensed data (WorldView-2, SPOT-6, and Senetinel-2A) were assessed on 70% ($n = 5603$) of the data. Although the RF has an internal evaluation system, we believe that the use of such a large independent sample dataset provides a more convincing evaluation of the classification. An error matrix was used in the study that uses overall accuracy, producer's accuracy, and user's accuracies statistics.[65] The user's accuracy indicates the probability that classified woody species and land cover types on the map represent the same category on the ground. This accuracy is thus calculated as the number of true observations of a class divided by the number of predicted observations. The producer's accuracy indicates the probability of a reference class being classified correctly, and it is calculated as the number of true observations of a class divided by the number of true reference observations of that class. Kappa coefficient statistic [Eq. (1)] was applied to evaluate the quality of classified imagery.[66] The kappa statistic is used to control the cases which might have been correctly classified by chance:

$$\text{Kappa coefficient} = \frac{P_{\text{observed}} - P_{\text{chance}}}{1 - P_{\text{chance}}}, \tag{1}$$

Table 2 Illustration of the number of woody plant species used for training and evaluation of classification.

Species name	Code	Leaf structure	Training	Validation
Acacia caffra	AC	Narrow-leaved	265	637
Acacia delabata	AD	Narrow-leaved	48	208
Acacia karro	AK	Narrow-leaved	177	252
Afrocanthium mundianum	AM	Narrow-leaved	120	160
Brachylaena rotundata	BR	Narrow-leaved	104	172
Celtis africana	CAf	Narrow-leaved	62	139
Celtis australis	CAu	Narrow-leaved	62	124
Cordyline australis	CA	Narrow-leaved	135	262
Dispyros natalensis	DN	Broad-leaved	50	284
Dombeya rotundifolia	DR	Broad-leaved	72	168
Ehretia rigida	ER	Narrow-leaved	103	207
Euclea crispa	EC	Narrow-leaved	75	138
Gymnosporia buxifolia	GB	Narrow-leaved	45	240
Heteromorpha arborescens	HA	Narrow-leaved	38	155
Kiggelaria africana	KA	Narrow-leaved	88	176
Melia azedarach	MA	Narrow-leaved	79	105
Olea europaea subs.africana	OEa	Narrow-leaved	66	175
Pittosporum viridiflorum	PV	Narrow-leaved	62	152
Populus x canescens	PC	Broad-leaved	36	147
Rhus lencia	RL	Narrow-leaved	59	141
Salix mucronata	SM	Narrow-leaved	104	151
Sambucus nigra	SN	Narrow-leaved	48	168
Searsia leptodictya	SL	Narrow-leaved	77	126
Searsia pyroides	SP	Narrow-leaved	67	157
Tarcchonanthus camphoratus	TC	Narrow-leaved	71	105
Zanthoxylum capense	ZC	Narrow-leaved	45	114
Ziziphus mucronata	ZM	Broad-leaved	70	184
Bareland	BL	No leaf	54	279
Grassland	GL	No leaf	73	133
Shrubs	SH	Mixed	53	144
Total	—	—	**2408**	**5603**

where $P_{observed}$ is the observed proportion of agreement and P_{chance} is the proportion expected by chance.

McNemar's test, which is a nonparametric and standardized normal test based on confusion matrices in a 2×2 dimension,[67] was also applied in this study. The McNemar's test computed

using Eq. (2) determines the binary distinction between correct and incorrect class designation by different images (Worldview-2, SPOT-6, and Sentinel-2A) using RF and SVM classifiers:

$$Z = \frac{f12 - f21}{\sqrt{f12 + f21}},$$ (2)

where the square of z follows a chi-square χ^2 distribution with 1 degree of freedom. $f12$ represents the misclassified number of samples by RF classifier using WorldView-2 but classified correctly by the same classifier using SPOT-6. $f21$ represents the total number of samples classified correctly by RF using WorldViw-2 but not classified correctly by RF classifier using SPOT-6. This approach of pairwise comparison was applied to other images using SVM as well.

3 Results

3.1 Classification Accuracies Derived from WorldView-2, SPOT-6, and Sentinel-2A

Figure 3 shows visual comparisons of woody species and coexisting land cover types using Worldview-2, SPOT-6, and Sentinel-2A images classified using RF and SVM classifiers. Overall classification accuracies of species and coexisting land covers derived from the three images showed the best overall accuracy of 65% for WorldView-2 image, followed by Sentinel-2A and then SPOT-6 using the RF classification (Fig. 4). Similarly, the SVM returned classification accuracies derived from the three images in the same ranking order as the RF, although the SVM had a lower accuracy for each image. Kappa coefficient statistics derived from the same three images showed that WorldView-2 had the highest kappa coefficient value of 0.63 followed by Sentinel-2A and then SPOT-6 using the RF classifier (Fig. 4). The kappa values of the three images using the SVM classifier had the same ranking order as the RF classifier (Fig. 4).
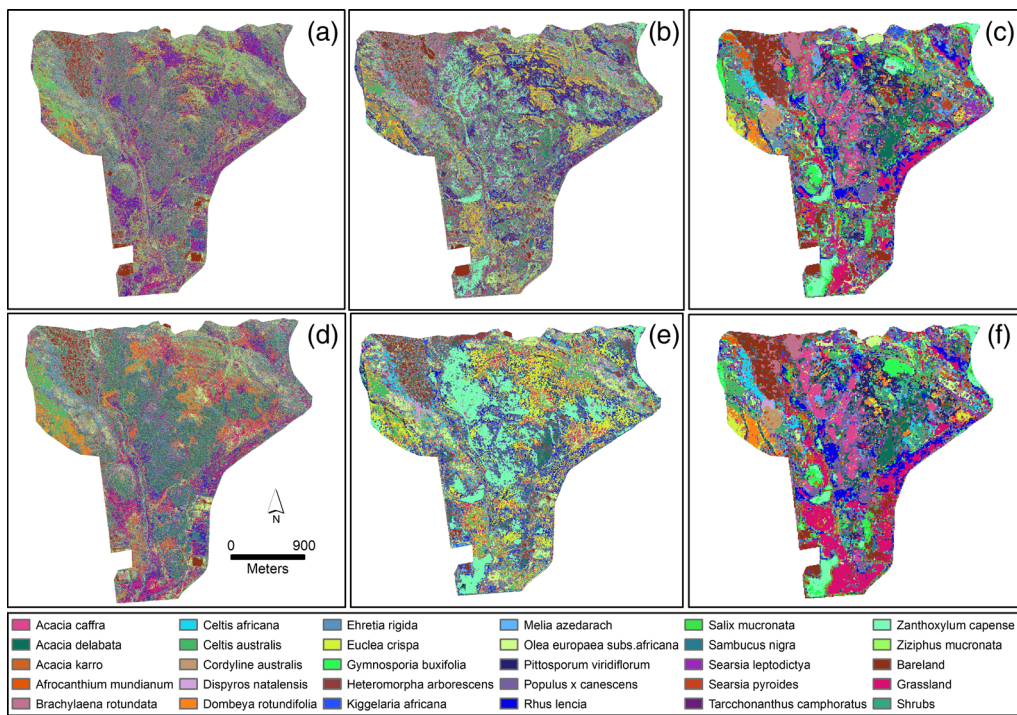
Fig. 3 Visual illustration on the performances of RF classification using (a) WorldView-2, (b) SPOT-6, and (c) Sentinel-2A; SVM classification using (d) WorldView-2, (e) SPOT-6, and (f) Sentinel-2A images in classifying woody plant species and coexisting land cover types.
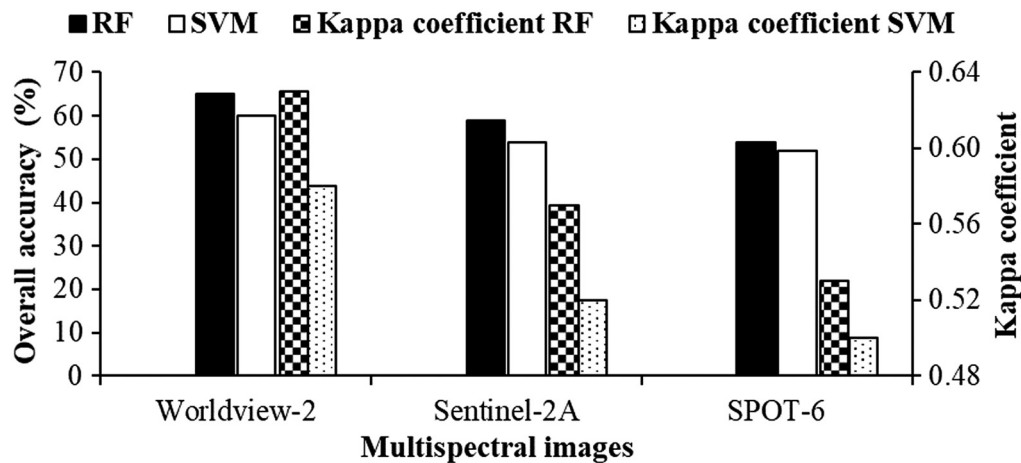
Fig. 4 Overall accuracies and kappa coefficient statistics for WorldView-2, Sentinel-2A, and SPOT-6 using RF and SVM classifiers.

Results from the McNemar's test revealed statistically significant difference between the accuracies of WorldView-2 ($\chi^2 = 9.15$; $p = 0.002$) and SPOT-6 ($\chi^2 = 6.34$; $p = 0.007$) when RF classification was used. The difference between Sentinel-2A ($\chi^2 = 4.48$; $p = 0.023$) and WorldView-2 images ($\chi^2 = 5.36$; $p = 0.034$) also were significant using the RF classifier. Such statistically significant difference was also observed between Sentinel-2A ($\chi^2 = 4.75$; $p = 0.042$) and SPOT-6 ($\chi^2 = 4.97$; $p = 0.048$). The SVM-based classification resulted in statistically significant difference between the accuracies of WorldView-2 ($\chi^2 = 7.15$; $p = 0.03$) and SPOT-6 ($\chi^2 = 8.34$; $p = 0.04$). Similarly, the differences between Sentinel-2A ($\chi^2 = 4.48$; $p = 0.023$) and WorldView-2 images ($\chi^2 = 5.36$; $p = 0.034$) were statistically significant using the SVM classifier. However, the differences between Sentinel-2A ($\chi^2 = 0.75$; $p = 0.142$) and SPOT-6 ($\chi^2 = 1.97$; $p = 0.248$) were statistically not significant using SVM.

Producer's and user's accuracies of individual plant species are shown in Fig. 5. The producer's accuracies ranged between 27% (*Cordyline australis*) and 83% (grassland) for different species across the three images when using the RF classifier [Fig. 5(a)]. When using WorldView-2 image and RF, 20 species and coexisting land covers had producer's accuracy exceeding 60% with 10 of them having 70% or higher accuracies. Sentinel-2A and RF combination yielded producer's accuracies of >60% for 15 species and coexisting land covers, while the accuracy exceeded 70% for seven species. Significantly, fewer species and coexisting land covers had good accuracies when SPOT-6 was used with only four species having >60% accuracies. The SVM classifier yielded producer's accuracies varying between 14% (*Heteromorpha arborescens*) and 94% (*Melia azedarach*) across the three images [Fig. 5(b)]. Specifically, WorldView-2 image returned producer's accuracies exceeding 60% for 16 species and exceeding 70% for seven species. The combination of Sentinel-2A and SVM resulted in quite low producer's accuracy with only eight species estimated at >60% accuracy while only two species scoring >70%. SPOT-6 and SVM combination fared better than SPOT-6 and RF combination but only marginally with six and three species having >60% and 70% accuracies, respectively. The user's accuracies ranged between 31% (grassland) and 95% (*Acacia caffra*) across the three images using RF [Fig. 5(c)] and from 11% (*H. arborescens*) to 92% (*A. caffra*) using SVM classifier [Fig. 5(d)]. Seventeen species and coexisting land covers had user's accuracy >60% and seven of those with >70% using WorldView-2 and RF combination [Fig. 5(c)]. For Sentinel-2A and RF combination, 13 species had user's accuracies exceeding 60% with five of those species having >70% accuracies. Using the SVM classifier, the numbers of species identified at accuracies >60% were significantly lower for the three images than what were obtained using the RF classifier; with the lowest performance observed for Sentinel-2A image (Fig. 5).

Using the producer's accuracy, which evaluates classification quality against the reference (truth), we can compare the relative performance of each image against the other two in identifying species (Fig. 6). The WorldView-2 was better than Sentinel-2A for 16 species and
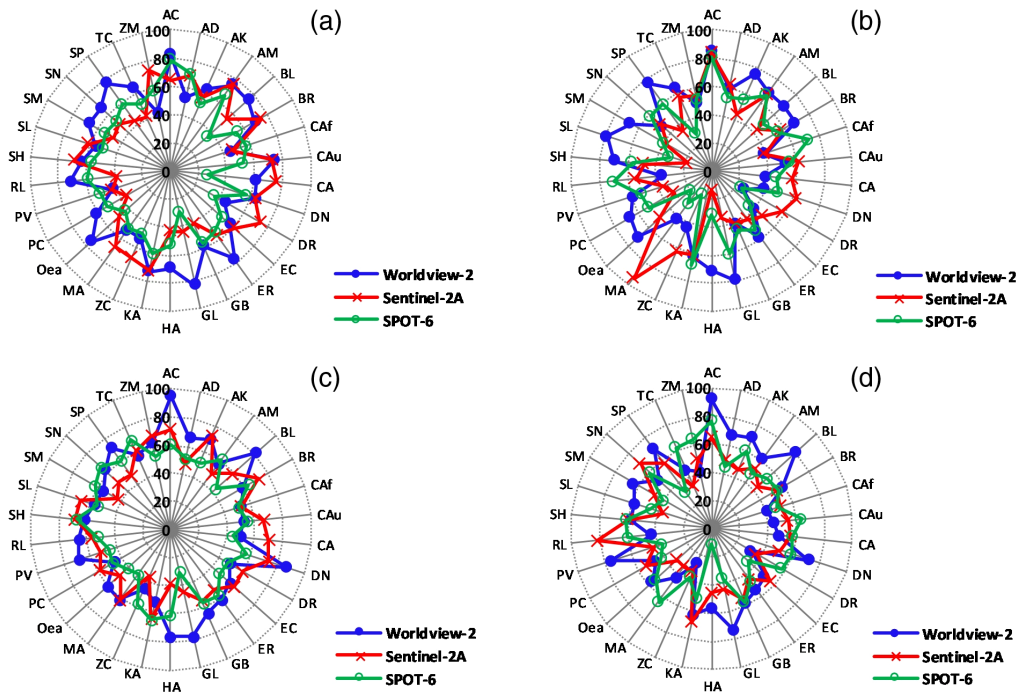
Fig. 5 Accuracies of identifying individual species using WorldView-2, Sentinel-2A, and SPOT-6; (a) RF producer's accuracy, (b) SVM producer's accuracy, (c) RF user's accuracy, and (d) SVM user's accuracy. Species names represented by the two-or three-letter codes are given in Table 2.
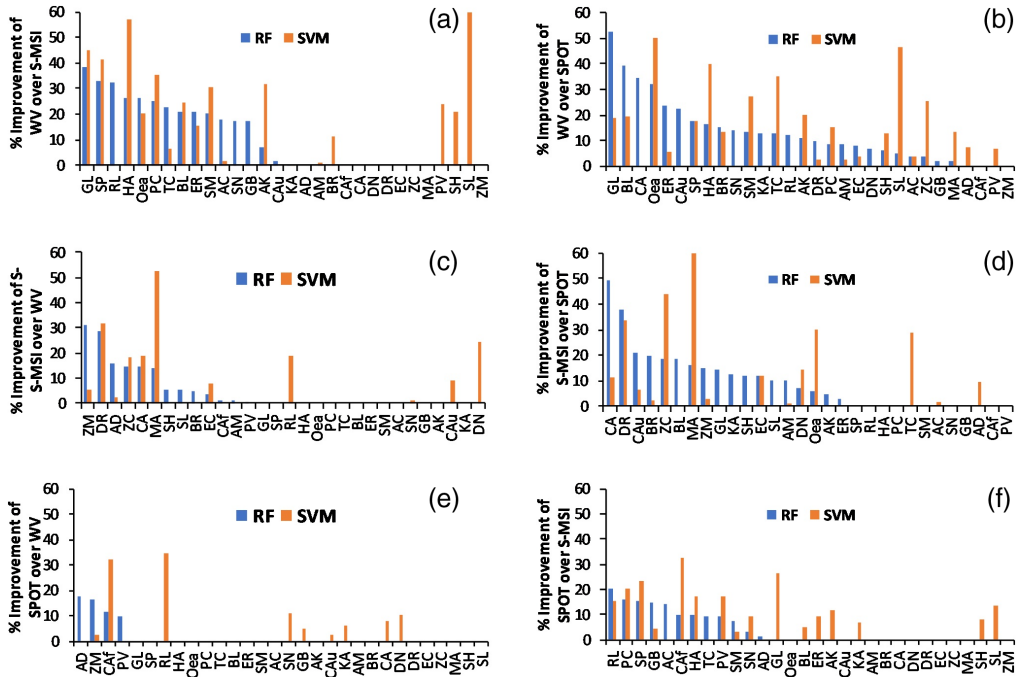
Fig. 6 Relative producer's accuracy of an image over the other images in identifying species types. Worldview-2 (WV), SPOT, and Sentinel-2A multispectral image (S-MSI) in the *y* axis represent satellite images. Species names represented by the two-or three-letter codes are given in Table 2.

coexisting land covers [Fig. 6(a)] with the relative improvement in producer's accuracy ranging between 1% and 38% for RF and 1% and 60% for SVM. The improvements exceeded 10% for 13 species using both classifiers. WorldView-2's improvement over SPOT-6 was even more for 26 and 21 species and coexisting land covers using RF and SVM, respectively [Fig. 6b], with the

improvement exceeding 10% for 15 or 14 species and coexisting land covers for the two classifiers. Notably, Sentinel-2A performed better than WorldView-2 for 13 (RF) and 11 (SVM) species with the improvement exceeding 10% for six species [Fig. 6(c)]. Sentinel-2A's better performance over SPOT-6 was observed for 18 and 14 species using the RF and SVM classifiers, respectively [Fig. 6(d)]. The relative performance of SPOT-6 over WorldView-2 was noted to be better in four or nine species depending on the classifier [Fig. 6(e)]. SPOT-6 was advantageous over Sentinel-2A for 12 or more species and coexisting land covers; this was the case more using the SVM than the RF classifier [Fig. 6(f)].

3.2 Comparison of Images Based on Confusions

It is useful to evaluate the level of confusion of a species against other species in a localized area with a diverse vegetation composition. Logically, the image that yields the smallest amount of confusion among coexisting species is considered desirable. Detailed confusion matrices using RF and SVM classification types are given in Table 3 in the Appendix A. Figure 7 provides the count of other species and coexisting land covers against which a species is confused. The RF classification clearly showed that the WorldView-2 identified nearly each of the species with the least number of confusions with other species. Using this image, a species is confused on average with 11 other species or land cover types, while 12 species were confused with <10 species and coexisting land covers [Fig. 7(a)]. In contrast, Sentinel-2A confused a species with an average of 18 species and coexisting land covers [Fig. 7(a)]. Despite an overall weaker performance of Sentinel-2A, it had comparable confusion level with WorldView-2 for certain species (e.g., *Acacia karro* and *Dispyros natalensis*) and fared better than WorldView-2 for three species (*Afrocanthium mundianum*, *C. australis*, and *Zanthoxylum capense*). SPOT-6 created considerable confusion in identifying each species at an average of 24 species and coexisting land covers confused with each species. The classification using SVM reduced the discrepancy among the three images, compared with the RF classifier [Fig. 7(b)]. In particular, the average number of species and coexisting land covers confused with any species was equal for WorldView-2 and Sentinel-2A at 16 while SPOT-6 confused a species with an average
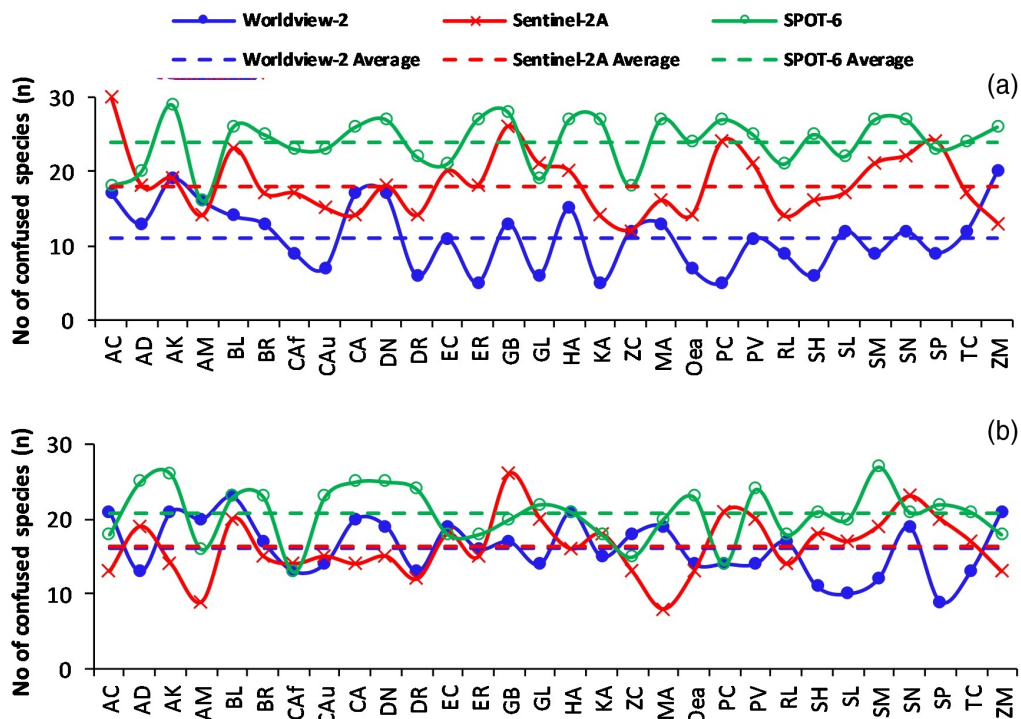
Fig. 7 Number of species confused against a given species for (a) RF and (b) SVM classifiers.

number of 21 species, which is an improvement from 24 species and coexisting land covers using the RF classifier. Notably, Sentinel-2A had a lower confusion rate than WorldView-2 for 16 species [Fig. 7(b)]—an improvement from only three species using the RF classifier [Fig. 7(a)].

While the above comparison focused on confusion based on the number of different species, it is important to compare images using the number of samples of each species that contributed significantly to inaccuracies. We illustrate this using a select species for both RF and SVM classifiers, and exhaustive confusions are given in Table 4 in the Appendix B. To balance the comparison across accuracies, we selected species from three producer's accuracy categories including <60%, 60% to 70%, and >75%. Since the intention was to compare images, the selected species in each category needed to satisfy the criterion using at least two images. The selection was made based on the results presented in Figs. 8(a) and 8(b), for the RF- and SVM-based producer's accuracies, respectively. Figure 8 illustrates three selected species including *A. caffra* (<60%), *A. karoo* (60% to 70%), and *Dombeya rotundifolia* (60% to 70%), and how their accuracies were affected largely by few species. Notable similarities were observed in terms of species type that contributed to inaccuracies of identifying each species; for instance, *A. caffra* was confused mainly with *A. karro*, *Afrocanthium mundianum*, *C. australis*, and grassland when using RF [Fig. 8(a)] and SVM [Fig. 8(b)]. It is also noteworthy to mention the agreement between the two classifiers in identifying the images with comparable confusions. For example, confusion of *A. caffra* with *A. karro* and *A. mundianum* was noted when Sentinel-2A and SPOT-6 were used exploiting RF and SVM classifiers. Although comparable images did not match consistently, certain similar observations can be seen in the identification of species. This can be noted for *A. karoo* whose inaccuracy was compromised by *A. caffra*, *Celtis australis*, and *Ehretia rigida* for both classifiers [Figs. 8(c) and 8(d)] while *D. rotundifolia* was confused mainly with *A. caffra* and *Ehretia rigida* for both classifiers [Figs. 8(e) and 8(f)].
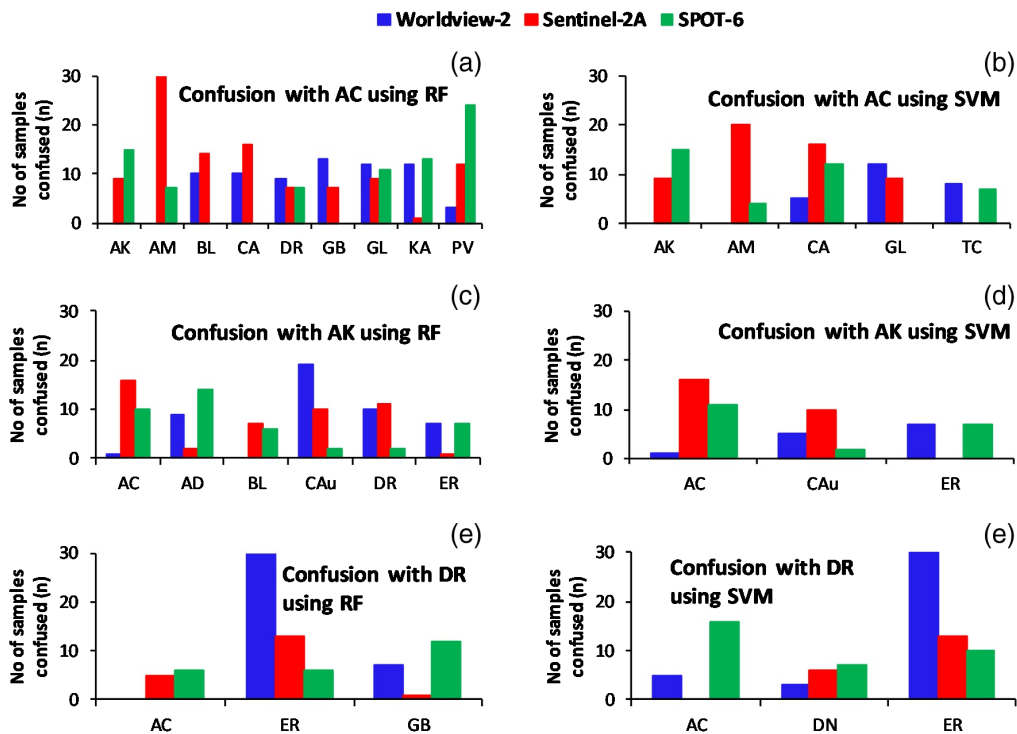
Fig. 8 Comparison of images based on number of samples contributing to confusions of three selected species: (a), (b) *A. caffra*, (c), (d) *A. karro*, and (e), (f) *D. rotundifolia* and using the RF and SVM classifiers.
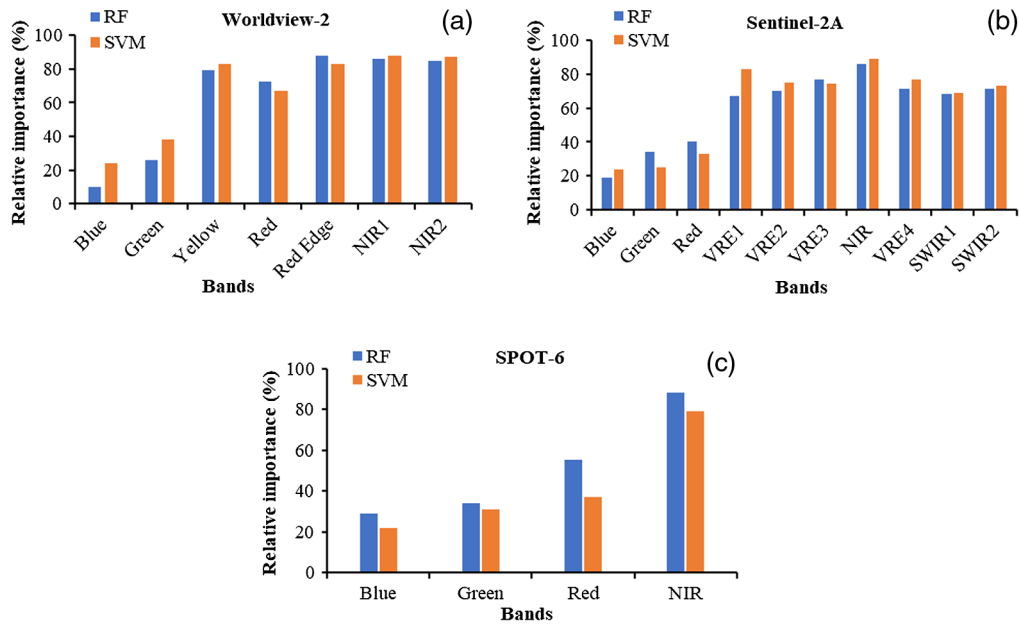
Fig. 9 The relative importance of the multispectral bands in classifying woody plant species using RF and SVM derived from (a) WorldView-2, (b) Sentinel-2A, and (c) SPOT-6 images; NIR, near-infrared; VRE, vegetation red edge; and SWIR, shortwave infrared band.

3.3 *Band Importance of WorldView-2, SPOT-6, and Sentinel-2A Images*

Variable importance, which measures the percentage that the prediction error increases when a predictor variable is removed, was computed for each image using both classifiers in an attempt to see the general trend in the contribution of individual bands [Figs. 9(a)–9(c)]. In general, there was a strong similarity among the three images in terms of the important regions of the electromagnetic spectrum for RF and SVM classifiers. Infrared range bands had the most contributions to the classifications for the three images (>50%) using both RF and SVM classifiers. For example, the near-infrared (NIR) band alone contributed to 65% or greater accuracy in all the images [Figs. 9(a)–9(c)]. There were also similarities among the three images in the contributions made by the blue and green bands each of which contributed to <40% accuracy. Further similarities can be noted between WorldView-2 and Sentinel-2A that have more spectral bands in the infrared wavelength regions. For example, each of NIR2 and red edge bands of WorldView-2 and VRE and SWIR bands of Sentinel-2A contributed >65% of the classifications. The SWIR1 and SWR2 available only in Sentinel-2A also made significant contributions to the classifications using both classifiers [Fig. 9(b)].

4 Discussion

4.1 *Performances of WorldView-2, SPOT-6, and Sentinel-2A*

Numerous studies have applied remotely sensed data with relatively low spectral and spatial characteristics failed to capture the true extent of localized plant species diversity.[34,41,68] Therefore, this study utilized WorldView-2, SPOT-6, and Sentinel-2A satellite images with improved spatial or spectral characteristics to capture several woody plant species and generic land cover types ($n = 30$) in a localized savanna environment during a dry season. WorldView-2 image yielded the highest overall classification accuracy (65%) using the RF classifier compared to other images (Fig. 4). One advantage of WorldView-2 data is the availability of a significant number of spectral bands present within a narrow spectral range.[69] Such property allows for improved discrimination of subtle differences among species in dry periods associated with low foliage, which may obscure characteristic differences between species.[40] The combination of improved spatial and spectral characteristics offered by WorldView-2 image reduces the mixed pixel problem inherent in coarser

spatial resolution and low spectral resolution images.[53,55] Variability in overall classification results of the three images might also have been influenced by different acquisition times of the three images. Although the images were all collected in dry period, even minor variations in weather conditions on different dates and times can result in variability of reflected radiation captured by the satellite images[70] thus contributing to a level of confusion in species identification.

Sentinel-2A image returned the second-best accuracy of discriminating the woody plant species and coexisting land covers in this study (overall accuracy = 59%). This accuracy is encouraging, given the relatively coarse spatial resolution of Sentinel-2A ($\geq$10 m) compared with WorldView-2 (65%) and considering the large number of species targeted in the study. Our study moderately agrees with Ref. 71 which used Sentinel-2A image to map 24 woody plant species and reported accuracies >65%. A key advantage of Sentinel-2 over WorldView-2 is that it has spectral bands in the SWIR region of the electromagnetic spectrum. Therefore, this advantage has compensated for the loss in the spatial resolution of the image. SPOT-6 imagery achieved the lowest accuracy (52%) of the three images used in the study. Although SPOT-6 imagery has relatively better spatial information compared with Sentinel-2A, it lacks detailed spectral bands particularly in the infrared regions that are suitable for differentiating plant species.[72] A similar inferior performance of SPOT image was reported by Ref. 34, which compared the accuracies of Landsat (50%) and SPOT-5 (30%) in the classification of plants in a savanna region in Australia. The producer's and user's accuracies generally corresponded with the overall accuracies in showing the superiority of WorldView-2 image over the others (Fig. 5). It is important to note that the above observations were somewhat similar for the RF and SVM classifiers, indicating the reliability of the findings in ranking the three images irrespective of a classification approach.

A comparison among the performance of the three images using relative improvement of producer's accuracies clearly showed the superiority of WorldView-2 image followed by Sentinel-2A and SPOT-6 as shown in Fig. 6. Specifically, the improvement of WorldView-2 over the other images in terms of producer's accuracy was evident for many species and coexisting land covers. The advantage of WorldView-2 over Sentinel-2A was also reported by Ref. 73, which estimated deciduous small spiral thin leaf oak plants ($n = 13$). It is noteworthy to mention the preference of Sentinel-2A over WorldView-2 for many species; this could be attributed to the image's spectral superiority. The vegetation type in the study area is dominated by narrow-leaved plant species (Table 2) and limited chlorophyll content due to the dry season conditions under which the data were collected. The combination of these factors necessitates the use of imagery that has multiple and narrow bands such as those found in Sentinel-2A.[32] The advantage of WorldView-2 over SPOT-6 agrees with Ref. 74 which reported better performance of WorldView-2 compared with SPOT-5 image in classifying plant species in a savanna vegetation environment, although they targeted fewer species ($n = 5$). Comparatively, SPOT-6 performed better than the other images for quite a few species [Figs. 6(e) and 6(f)], understandably due to the lower spectral qualities it possesses compared with the other images.

4.2 Confusion Levels of Images

In most cases, the classification using WorldView-2 (as opposed to the other images) resulted in each species confused with the least number of different species particularly when the RF classifier was used [Fig. 6(a)]. The weakness of Sentinel-2A in this regard can be attributed to the physiological characteristics of the vegetation in the study area of which >90% of species type are narrow-leaved plants such as *H. arborescens*, *A. karro, C. australis*, etc. Narrow-leaved plant species are difficult to discriminate using images with coarse spatial resolution images[34,71] such as the Sentinel-2A (10 to 60 m, spatial resolution) used in this study. Although SPOT-6 has a relatively high spatial resolution, it still resulted in confusion among several species as well as coexisting land cover types. It is important to note that deciduous species identified in the study area lose their leaves during the winter period when the data for this study were collected.[45] The limited spectral capability offered by SPOT-6 is unlikely to differentiate species accurately. Although SPOT-6 imagery has better spatial information than Sentinel-2A, the results show that spatial information alone is insufficient to discriminate woody plant species accurately.

It is worth noting that the SVM classifier applied to Sentinel-2A resulted in lower misclassification of each species with other species when compared with the RF classifier. In fact,

the improvement in general showed similarity of the image with WorldView-2. This can be attributed to the spectral advantages of Sentinel-2A which divides the red-edge region into four bands.[75] The performance of Sentinel-2A comparable to WorldView-2's is encouraging since the former is widely and publicly available at no cost.

In identifying a species in a highly diverse savanna ecosystem, it is critical to pinpoint species that have major contributions to misclassifications of a target species. The findings of this study showed that few species created most of the confusions in the classification of the 27 woody plant species, and these confusions are evidenced by at least two of the three images (Fig. 8). Such confusions can be attributed to the similarity in foliage (leaf) characteristics of the species inducing somewhat similar spectral responses captured by the three sensors in the study.[73] This suggests, among others, the need for advanced remote sensing systems with spectral and spatial characteristics better than those used in this study.

4.3 *Comparison of Images Based on Band Importance*

Comparison of variable importance findings showed that the highest contributions from all the three images in the analysis (WorldView-2, SPOT-6, and Sentinel-2A) and classifiers (RF and SVM) were made by the infrared bands (Fig. 9). This finding is in agreement with Refs. 76 to 79 who discriminated narrow-leaved plant species in a savanna environment. The yellow band of WorldView-2 image performed also performed well comparatively to infrared bands. This is expected since the band is useful in detecting woody plant species with gray to yellow coloring often present during dry periods in savanna environments.[68] The significant contribution of the red-edge band available in WorldView-2 and Sentinel-2A is related to the sensitivity of the band to chlorophyll variations of even small narrow-leaved plants.[80] The availability and significant contributions of vegetation red edge bands in Sentinel-2A clearly places it at advantage over Landsat imagery, which largely shares similar spatial and spectral characteristics with Sentinel-2A.

5 Conclusions

This study compared WorldView-2, Sentinel-2A, and SPOT-6 images to detect several woody plant species in a savanna environment during a dry season. The image with the best spatial and spectral characteristics (WorldView-2) performed better compared with Sentinel-2A and SPOT-6 images. The findings highlighted the effectiveness of multispectral images in detecting woody plant species with similar foliage (or leaf) characteristics, although the level of greenness desired in vegetation characterization using remote sensing was generally low. A comparative look at the three images showed WorldView-2 to be the best followed closely by Sentinel-2A, which is available publicly at no cost. The comparability between the two images can be attributed to the higher spatial resolution offered by WorldView-2 and better spectral qualities of Sentinel-2A. The superiority in spectral qualities of Sentinel-2A resulted in the classification accuracies that were better than those obtained using SPOT-6 which has a better spatial resolution but significantly lower spectral qualities devoid of details in infrared regions of the electromagnetic spectrum. While the results of this study are quite promising, it is important to acknowledge the need for improved spatial and spectral resolutions to inform efficient species diversity monitoring strategies.

6 Appendix A: Classifier error matrix of WorldView-2, Sentinel-2A, and SPOT-6 images using the RF classifier

Error matrix provides detailed description of the confusion in species classification using WorldView-2, Sentinel-2A, and SPOT-6 images and RF classifier (Table 3).

7 Appendix B: Classifier error matrix of WorldView-2, Sentinel-2A, and SPOT-6 images using the SVM classifier

Error matrix provides detailed description of the confusion in species classification using WorldView-2, Sentinel-2A and SPOT-6 images, and SVM classifier (Table 4).

Table 3. Error matrix of three images using Random Forest.

REF / RF

PRED	Sensor	AC	AD	AK	AM	BL	BR	CAf	CAu	CA	DN	DR	EC	ER	GB	GL	HA	KA	ZC	MA	Oea	PC	PV	RL	SH	SL	SM	SN	SP	TC	ZC	ZM
AC	WV	524	4	1	1	0	1	2	0	5	0	0	0	0	0	10	0	0	1	1	0	0	0	0	0	0	0	0	0	0	0	1
	Sentinel	410	7	16	8	15	4	0	4	8	6	5	2	5	10	0	0	3	0	0	10	1	19	4	4	6	10	1	5	9	6	4
	SPOT	501	9	10	4	20	15	12	12	13	24	6	9	11	16	1	14	13	5	10	8	17	14	5	16	10	11	12	13	7	10	16
AD	WV	4	110	9	5	0	4	3	0	5	0	0	0	0	0	0	0	0	5	4	0	0	12	0	0	0	0	0	0	0	0	4
	Sentinel	15	143	2	3	0	4	13	2	8	4	1	1	0	2	4	12	0	0	2	12	13	21	30	0	2	4	2	1	0	2	0
	SPOT	4	146	14	9	11	1	0	2	18	7	3	4	3	1	1	0	2	5	4	14	1	2	10	1	5	6	4	3	1	5	4
AK	WV	0	8	160	3	0	5	11	3	5	3	4	0	2	0	0	0	0	4	6	0	1	0	8	0	0	1	0	3	0	0	1
	Sentinel	9	1	143	1	7	0	0	5	0	2	0	0	6	3	0	4	6	0	0	1	0	0	0	0	1	0	1	3	0	1	3
	SPOT	15	5	132	5	6	3	7	7	3	7	4	0	3	10	0	4	3	5	3	5	8	0	0	1	7	4	2	3	1	7	1
AM	WV	0	13	5	120	0	3	2	1	8	3	0	2	0	0	0	3	0	12	0	0	0	15	13	0	0	2	2	2	0	0	3
	Sentinel	30	1	2	122	2	1	0	1	0	8	7	2	0	1	1	1	0	7	2	6	7	2	5	3	3	0	0	4	9	3	15
	SPOT	7	4	3	106	2	1	0	0	2	6	0	2	1	5	0	0	2	0	1	10	0	1	0	2	1	2	0	3	3	1	9
BL	WV	10	0	0	0	171	4	0	0	0	0	0	0	0	0	2	1	0	0	5	0	0	0	0	0	5	0	0	10	3	5	0
	Sentinel	14	0	7	1	151	1	10	0	2	0	6	2	10	2	8	13	0	0	0	0	5	2	0	2	8	2	6	1	2	8	0
	SPOT	0	10	6	2	100	7	4	3	5	12	3	5	10	2	7	9	3	5	1	1	3	1	3	5	6	3	5	7	3	6	0
BR	WV	3	1	10	6	1	120	3	14	0	0	0	0	0	0	0	0	0	13	4	3	0	0	4	0	0	0	0	0	2	0	9
	Sentinel	4	0	0	0	1	128	2	0	0	2	0	0	0	1	3	2	0	0	0	14	1	1	0	2	0	1	1	3	9	6	0
	SPOT	0	0	12	0	4	94	0	3	4	0	3	0	3	1	0	3	0	2	2	2	2	4	0	0	0	1	2	1	1	0	1

Table 3. (*Continued*).

	PRED	AC	AD	AK	AM	BL	BR	CAf	CAu	CA	DN	DR	EC	ER	GB	GL	HA	KA	ZC	MA	Oea	PC	PV	RL	SH	SL	SM	SN	SP	TC	ZC	ZM
WV	CAf	0	2	11	1	1	6	63	0	24	0	0	0	0	0	0	2	0	0	0	0	0	0	0	0	0	0	8	0	0	0	2
Sentinel		3	0	4	0	2	3	65	0	0	0	1	1	1	4	0	6	0	1	0	1	4	0	1	0	4	9	3	8	3	4	0
SPOT		6	0	2	0	28	0	79	3	2	2	1	2	1	2	0	2	1	0	0	3	4	3	2	1	1	3	3	2	1	1	2
WV	CAu	0	3	19	2	1	10	0	92	34	2	0	0	0	0	0	2	0	2	0	0	0	0	0	0	0	0	9	0	0	0	0
Sentinel		3	0	10	0	4	0	5	90	0	2	0	0	0	3	0	0	0	0	2	0	7	1	0	0	0	1	1	0	7	0	0
SPOT		6	0	2	1	4	0	2	64	1	4	1	3	3	2	3	3	2	0	1	4	0	2	1	1	2	2	1	0	1	2	3
WV	CA	10	30	3	1	32	5	27	9	160	15	0	10	0	0	0	1	0	4	0	0	0	0	9	0	0	0	2	0	0	0	6
Sentinel		16	18	0	5	2	0	0	0	199	0	0	0	1	11	1	5	0	9	1	2	9	1	0	2	2	2	0	0	0	0	0
SPOT		0	3	1	2	0	1	8	4	70	6	2	15	4	8	0	2	2	1	2	5	3	1	3	1	2	1	3	3	3	2	4
WV	DN	0	0	1	2	0	0	0	0	3	180	3	0	0	0	0	2	0	0	0	0	0	0	0	0	0	0	15	0	1	0	2
Sentinel		7	10	4	1	1	9	0	2	0	180	2	1	1	0	10	4	0	0	1	0	2	6	0	0	1	0	0	5	5	1	0
SPOT		12	3	8	0	20	4	1	3	8	160	7	2	8	3	1	3	3	2	2	4	1	4	3	6	1	4	5	4	1	1	2
WV	DR	9	0	10	0	0	0	0	0	2	14	76	0	33	0	0	0	0	0	0	0	0	5	1	0	0	0	5	0	0	0	1
Sentinel		7	1	11	0	9	0	8	0	2	3	124	0	13	3	0	10	3	4	1	0	2	0	0	0	4	0	1	3	2	4	0
SPOT		7	1	2	1	4	2	0	1	2	2	60	4	6	6	0	1	1	0	2	4	2	2	3	4	3	3	3	2	0	3	0
WV	EC	12	0	1	0	17	0	0	0	2	0	0	79	0	0	9	0	0	1	10	0	0	0	0	0	1	0	0	5	1	1	2
Sentinel		3	1	0	1	0	1	1	1	0	1	0	84	4	8	6	5	8	0	0	0	3	5	0	0	2	0	0	3	2	2	1
SPOT		2	3	2	0	1	3	1	1	23	2	0	68	1	3	23	0	1	0	0	1	3	1	0	0	0	0	2	0	1	0	4

Table 3. (*Continued*).

REF	PRED	AC	AD	AK	AM	BL	BR	CAf	CAu	CA	DN	DR	EC	ER	GB	GL	HA	KA	ZC	MA	Oea	PC	PV	RL	SH	SL	SM	SN	SP	TC	ZC	ZM
ER	WV	0	0	7	0	0	0	0	0	0	3	77	2	160	5	0	1	0	0	0	0	0	3	0	0	0	0	0	0	0	0	1
	Sentinel	21	0	1	0	34	0	0	0	0	2	13	0	117	0	8	3	2	2	4	0	0	0	3	0	5	0	0	6	0	5	0
	SPOT	0	3	7	1	0	4	1	0	3	7	6	7	111	7	4	2	1	0	1	4	1	3	2	1	3	3	3	4	1	3	2
GB	WV	13	0	0	0	0	0	0	0	0	20	7	0	0	140	0	0	9	0	0	0	0	0	0	14	0	0	0	6	0	0	6
	Sentinel	7	1	3	3	1	0	4	5	0	0	1	2	0	99	0	7	0	1	10	0	6	6	10	1	0	4	3	2	2	0	1
	SPOT	0	4	2	0	4	7	2	4	3	7	12	5	6	135	2	4	3	1	0	2	1	5	6	4	4	2	3	5	1	4	2
GL	WV	12	0	0	0	1	0	0	0	0	0	0	0	10	2	110	0	0	0	0	0	0	0	1	0	0	0	0	0	5	0	0
	Sentinel	9	2	3	0	1	1	0	4	1	4	0	10	6	2	59	0	15	0	1	0	9	1	0	0	0	1	0	2	0	1	1
	SPOT	11	0	5	1	13	1	1	2	22	3	5	1	5	3	40	1	1	1	1	2	2	0	1	1	1	2	0	2	0	1	1
HA	WV	0	0	2	0	0	0	0	0	1	3	0	0	0	0	0	100	0	0	0	0	0	0	0	0	6	13	4	0	2	6	0
	Sentinel	21	2	3	0	12	0	3	1	0	0	0	1	2	2	3	66	1	4	1	1	8	1	2	7	3	7	10	1	4	3	5
	SPOT	0	2	1	0	5	4	2	0	1	3	11	0	0	1	0	76	2	0	1	0	1	3	0	1	2	1	2	3	0	2	2
KA	WV	12	0	0	1	3	0	0	0	2	5	0	0	2	10	0	0	129	0	6	10	35	7	2	18	0	0	0	0	0	0	1
	Sentinel	1	0	1	0	0	0	0	1	0	0	0	9	2	21	5	0	128	2	1	0	2	0	10	1	0	4	6	2	0	0	2
	SPOT	13	2	3	2	0	2	1	1	0	1	0	2	1	3	2	2	106	0	2	0	2	4	0	3	0	2	2	2	3	0	0
ZC	WV	2	11	2	5	0	0	0	0	6	0	0	8	0	0	0	3	0	60	0	0	0	0	0	0	0	0	0	0	7	0	26
	Sentinel	13	3	1	0	13	1	5	0	30	2	2	2	11	3	3	5	1	77	3	4	1	2	6	3	6	3	8	2	0	6	2
	SPOT	0	0	1	1	13	0	0	0	0	0	0	1	2	0	0	2	1	56	1	3	2	2	6	1	0	1	0	1	1	0	2

Table 3. (Continued).

PRED		REF RF	AC	AD	AK	AM	BL	BR	CAf	CAu	CA	DN	DR	EC	ER	GB	GL	HA	KA	ZC	MA	Oea	PC	PV	RL	SH	SL	SM	SN	SP	TC	ZC	ZM
MA	WV		0	0	0	0	5	1	0	0	0	0	0	3	0	6	0	0	0	0	55	0	0	0	3	0	1	0	0	4	3	1	8
	Sentinel		4	1	0	0	0	1	1	4	0	0	1	3	1	10	3	4	0	0	70	0	1	0	1	5	1	0	2	1	0	1	0
	SPOT		10	0	5	0	11	4	4	2	1	1	18	0	1	2	3	0	3	0	53	2	1	3	1	0	0	1	6	0	2	0	1
OEa	WV		12	0	2	0	0	0	0	0	1	10	0	0	0	8	0	2	14	0	0	131	17	3	0	18	0	0	0	0	0	0	0
	Sentinel		2	5	0	0	0	3	0	0	0	23	0	2	10	2	0	1	2	4	0	85	1	5	11	0	0	11	6	1	0	0	1
	SPOT		0	2	4	0	3	1	2	1	33	0	6	1	4	1	0	0	3	5	3	75	3	3	5	0	2	3	3	2	6	2	10
PC	WV		0	0	1	1	5	0	0	0	0	0	0	0	0	10	1	0	11	0	3	16	89	29	0	0	1	0	0	0	0	1	25
	Sentinel		3	0	0	0	3	0	3	0	0	2	0	1	0	10	1	3	1	0	0	0	52	4	0	0	0	0	3	1	2	0	1
	SPOT		8	0	2	0	4	4	2	1	20	5	0	3	3	3	3	1	3	0	2	3	76	1	1	2	0	1	1	3	5	0	2
PV	WV		3	3	0	7	0	0	0	0	0	6	0	0	0	0	0	0	0	0	0	0	0	65	0	0	1	4	0	0	1	1	5
	Sentinel		12	0	0	0	2	0	3	0	2	0	0	1	10	12	1	2	0	1	0	0	0	66	0	0	0	3	7	0	4	0	0
	SPOT		24	0	3	0	8	3	4	2	7	2	2	1	4	4	5	4	4	1	2	0	2	80	1	2	1	1	3	1	2	1	1
RL	WV		0	7	1	1	0	0	10	4	2	0	0	12	0	0	0	5	0	3	1	1	0	0	100	0	0	0	1	0	0	0	0
	Sentinel		3	0	0	0	2	0	0	2	0	8	0	0	0	21	1	1	0	0	0	0	0	1	54	1	1	0	0	1	0	0	0
	SPOT		3	1	6	0	1	1	0	0	5	5	0	0	3	4	27	2	3	9	1	1	1	0	83	0	0	0	2	0	0	0	1
SH	WV		2	0	0	0	0	0	0	0	0	1	0	0	0	28	0	0	13	0	0	10	0	0	0	91	0	0	0	1	0	0	1
	Sentinel		2	0	3	0	3	0	0	0	1	0	0	0	0	2	2	1	0	0	1	0	1	2	0	99	0	5	5	13	1	0	3
	SPOT		2	1	0	1	1	1	0	1	4	2	2	0	1	0	2	1	0	1	2	2	1	0	2	82	3	2	2	1	4	3	1

Table 3. (*Continued*).

PRED			REF (RF)																															
		AC	AD	AK	AM	BL	BR	CAf	CAu	CA	DN	DR	EC	ER	GB	GL	HA	KA	ZC	MA	Oea	PC	PV	RL	SH	SL	SM	SN	SP	TC	ZC	ZM
WV	SL	3	0	2	0	3	7	0	0	0	5	0	4	0	2	0	3	0	0	1	0	0	2	0	0	70	15	2	3	1	70	0
Sentinel		4	0	0	0	9	1	0	0	2	0	2	0	6	4	3	0	0	0	4	0	0	0	0	0	77	1	0	1	1	77	0
SPOT		0	1	7	1	6	2	3	2	6	1	0	1	1	3	3	2	0	0	1	0	1	2	0	2	64	3	1	1	1	64	2
WV	SM	2	0	0	0	21	0	0	0	0	0	0	2	0	13	0	15	0	0	0	0	0	1	0	0	12	101	6	0	11	12	0
Sentinel		3	2	33	1	2	3	1	0	0	20	0	1	0	1	0	0	1	0	0	4	1	0	0	2	1	70	7	7	0	1	0
SPOT		0	0	3	2	4	3	1	1	0	2	6	0	3	4	1	1	2	2	1	0	4	3	1	1	1	81	1	0	1	1	2
WV	SN	4	2	0	1	0	0	18	1	1	5	0	5	0	1	0	0	0	2	0	4	0	0	0	1	6	11	111	0	0	6	3
Sentinel		4	3	2	2	1	2	6	1	2	0	0	6	0	2	3	0	4	0	0	5	4	4	2	2	0	5	82	7	4	0	12
SPOT		0	1	3	0	1	2	0	1	3	2	1	2	4	4	0	3	2	1	2	2	1	2	1	1	1	0	87	3	1	1	0
WV	SP	0	0	0	0	8	0	0	0	0	3	0	11	0	12	0	2	0	0	8	0	0	0	0	2	1	0	0	120	0	1	0
Sentinel		3	2	0	0	2	3	8	1	1	12	1	6	1	0	4	0	0	2	1	3	2	0	2	10	1	5	5	68	0	1	0
SPOT		4	2	2	0	4	0	0	0	2	1	5	2	4	4	4	2	4	1	1	1	0	5	1	2	3	4	2	92	0	3	1
WV	TC	0	0	0	0	1	1	0	0	0	6	1	0	0	3	1	3	0	0	1	0	0	0	0	0	13	3	0	7	67	13	0
Sentinel		3	0	0	1	0	5	1	0	1	3	0	0	0	1	4	0	1	0	0	0	0	1	0	1	0	2	2	2	44	0	0
SPOT		0	0	1	0	1	0	1	0	1	3	0	0	0	1	0	1	4	0	0	0	1	1	0	0	0	2	5	0	54	0	1
WV	SM	2	0	0	0	21	0	0	0	0	0	0	2	0	13	0	15	0	0	0	0	0	1	0	0	12	101	6	0	11	111	0
Sentinel		3	2	33	1	2	3	1	0	0	20	0	1	0	1	0	0	1	0	0	4	1	0	0	2	1	70	7	7	0	82	0
SPOT		0	0	3	2	4	3	1	1	0	2	6	0	3	4	1	1	2	2	1	0	4	3	1	1	1	81	1	0	1	87	2

Table 3. (Continued).

PRED		AC	AD	AK	AM	BL	BR	CAf	CAu	CA	DN	DR	EC	ER	GB	GL	HA	KA	ZC	MA	Oea	PC	PV	RL	SH	SL	SM	SN	SP	TC	ZC	ZM
WV	ZC	0	14	5	3	0	0	0	0	1	0	0	0	0	0	0	0	0	7	0	0	5	10	0	0	0	1	0	0	0	0	77
Sentinel		1	5	3	10	0	2	0	0	3	0	2	1	0	0	0	0	0	0	0	27	5	1	0	1	0	1	0	2	0	0	134
SPOT		2	5	3	21	0	2	1	3	0	7	4	0	0	2	1	0	1	11	2	17	3	0	0	1	3	3	2	0	0	3	107
WV	ZM	12	0	2	0	0	0	0	0	1	10	0	0	0	8	0	2	14	0	0	131	17	3	11	18	0	0	0	0	0	0	0
Sentinel		2	5	0	0	0	3	0	0	0	23	0	2	10	2	0	1	2	4	0	85	1	5	11	0	0	11	6	1	1	0	1
SPOT		0	2	4	0	3	1	2	1	33	0	6	1	4	1	0	0	3	5	3	75	3	3	5	0	2	3	3	2	6	2	10

Table 4. Error matrix of three images using Support Vector Machine.

PRED		AC	AD	AK	AM	BL	BR	CAf	CAu	CA	DN	DR	EC	ER	GB	GL	HA	KA	ZC	MA	Oea	PC	PV	RL	SH	SL	SM	SN	SP	TC	ZC	ZM
AC	WV	541	4	1	1	0	1	9	0	5	0	5	2	0	1	1	1	6	2	1	0	0	1	0	0	1	0	3	0	0	1	3
	Sentinel	531	7	16	8	15	4	0	0	0	0	0	2	0	10	0	0	0	1	0	17	3	16	15	10	6	15	1	5	12	0	1
	SPOT	519	9	11	4	0	1	12	5	13	24	16	9	11	8	1	14	13	5	10	8	17	14	0	16	12	11	0	13	7	20	0
AD	WV	4	125	2	5	0	4	3	0	5	0	0	2	1	0	0	0	2	5	4	0	0	6	9	1	0	0	3	0	0	4	3
	Sentinel	15	130	2	30	0	3	9	0	8	4	1	1	0	2	0	12	0	0	0	14	15	18	7	9	2	4	2	1	0	0	2
	SPOT	0	110	14	9	12	3	0	2	18	7	0	4	0	1	1	0	2	4	4	14	0	2	0	1	2	6	4	0	1	4	4
AK	WV	0	8	190	3	0	0	19	3	5	3	4	0	2	0	0	0	0	4	6	6	4	0	8	0	0	1	3	0	0	0	3
	Sentinel	9	1	110	1	28	3	0	3	0	12	0	0	0	3	0	4	3	0	0	1	0	0	0	0	1	0	1	3	0	1	1
	SPOT	15	5	140	5	6	3	7	9	0	2	0	1	0	22	3	26	3	23	0	5	8	0	0	2	7	4	2	3	1	3	2
AM	WV	0	1	5	110	2	1	2	1	8	3	0	5	0	0	0	3	0	11	3	0	0	5	13	0	0	2	2	0	0	0	2
	Sentinel	20	1	2	108	2	1	0	1	0	8	3	2	0	1	2	1	10	3	0	6	3	2	12	3	3	6	4	9	12	0	4
	SPOT	4	4	3	106	0	1	0	0	2	6	4	2	20	23	2	0	2	0	0	10	0	0	0	3	1	2	0	3	3	0	0
BL	WV	10	0	0	0	186	4	2	0	0	0	2	1	0	0	2	1	0	1	5	0	0	0	0	0	5	0	0	10	3	0	0
	Sentinel	0	5	7	0	123	1	10	0	2	0	0	2	32	2	8	13	0	0	0	0	5	2	1	2	8	2	6	0	2	0	6
	SPOT	8	10	3	2	138	7	4	2	0	20	4	8	10	2	7	0	3	32	0	1	16	2	3	5	6	3	5	7	3	0	5
BR	WV	3	1	5	2	6	117	3	15	0	0	0	0	3	0	0	0	0	12	4	3	0	0	4	0	9	0	6	1	2	6	6
	Sentinel	0	0	10	0	0	98	32	0	0	0	0	0	0	1	6	3	3	0	0	0	1	1	0	6	0	1	3	0	6	12	3
	SPOT	0	0	12	0	0	94	0	3	4	0	4	9	15	0	3	3	0	2	2	12	0	4	0	2	0	1	2	1	1	1	2

Table 4. (Continued).

	PRED	AC	AD	AK	AM	BL	BR	CAf	CAu	CA	DN	DR	EC	ER	GB	GL	HA	KA	ZC	MA	Oea	PC	PV	RL	SH	SL	SM	SN	SP	TC	ZC	ZM
WV	CAf	3	2	7	1	1	1	55	6	24	0	1	3	0	0	3	2	2	2	1	0	0	0	9	0	0	0	8	0	0	2	8
Sentinel		3	0	4	0	2	3	55	0	0	0	4	1	1	4	1	0	1	0	0	1	15	0	0	0	4	9	3	0	3	0	3
SPOT		6	5	2	0	10	0	100	0	6	12	1	2	1	2	0	21	0	0	0	8	4	0	2	1	1	3	3	2	3	0	3
WV	CAu	0	3	5	2	1	0	0	66	34	2	0	0	21	0	0	2	0	2	0	1	0	0	0	1	0	0	9	0	0	0	9
Sentinel		0	0	10	0	4	0	0	77	0	2	0	0	0	3	0	0	1	0	0	0	7	6	0	0	0	1	1	0	8	0	1
SPOT		6	0	2	1	9	0	0	69	1	4	9	6	0	0	3	0	0	0	0	0	0	2	1	4	3	1	0	0	3	3	0
WV	CA	5	30	3	1	3	0	15	9	100	15	1	3	0	0	0	3	0	4	0	0	0	0	9	0	0	0	3	0	0	6	3
Sentinel		16	6	0	5	9	0	1	0	150	0	0	0	29	11	2	0	13	8	0	3	3	1	0	2	0	2	0	0	0	0	0
SPOT		12	3	1	2	1	1	0	4	120	6	2	15	4	8	2	2	0	1	0	12	0	1	3	1	3	1	3	2	3	0	3
WV	DN	0	0	1	2	3	0	0	0	3	111	3	0	0	0	1	2	0	0	5	2	2	0	0	0	0	0	15	0	1	2	15
Sentinel		0	10	4	0	21	16	0	2	0	180	6	1	1	0	10	0	0	0	0	0	0	6	5	8	1	15	0	0	5	13	0
SPOT		0	3	6	0	12	4	1	3	8	140	7	12	9	0	1	2	3	0	0	4	9	4	3	6	0	4	5	4	23	2	5
WV	DR	9	0	2	0	0	2	0	3	2	14	44	0	33	0	0	1	3	0	0	0	0	5	11	0	0	0	5	0	0	3	5
Sentinel		0	1	11	0	9	0	8	0	2	3	97	0	13	3	0	10	3	0	1	0	0	0	0	0	4	0	1	3	2	0	1
SPOT		0	6	2	1	4	2	0	2	2	2	40	4	6	6	2	1	0	0	12	0	5	0	0	0	3	3	3	2	0	1	3
WV	EC	12	0	1	0	0	0	0	0	2	0	0	55	0	0	3	0	0	1	1	0	0	0	10	6	1	0	0	5	1	2	0
Sentinel		3	10	0	0	0	0	0	1	0	0	0	66	4	8	6	45	6	0	0	0	12	10	0	0	2	0	0	3	2	13	0
SPOT		0	3	2	0	1	3	0	1	0	2	0	50	1	23	1	0	1	0	0	0	0	1	0	0	0	0	0	0	0	0	0

Table 4. (Continued).

PRED		AC	AD	AK	AM	BL	BR	CAf	CAu	CA	DN	DR	EC	ER	GB	GL	HA	KA	ZC	MA	Oea	PC	PV	RL	SH	SL	SM	SN	SP	TC	ZC	ZM
ER	WV	3	0	7	0	0	0	0	0	0	3	77	2	120	5	0	1	1	0	0	0	0	3	0	0	0	0	0	0	0	1	0
	Sentinel	0	0	0	0	34	0	0	0	13	12	13	0	88	0	8	3	2	0	0	0	0	0	3	0	5	0	0	0	6	0	0	0
	SPOT	7	3	7	1	12	8	1	0	3	7	10	7	108	7	4	2	0	0	1	23	0	3	2	0	7	3	3	4	0	9	3
GB	WV	1	0	0	0	5	2	0	2	0	20	7	0	0	98	0	0	1	2	3	3	5	0	0	3	0	0	5	6	0	6	5
	Sentinel	0	0	0	3	1	0	4	5	0	0	3	2	0	99	4	23	0	1	0	0	6	9	0	1	0	3	3	2	2	3	3
	SPOT	11	4	2	0	4	7	2	4	3	7	2	5	0	110	2	4	3	1	0	2	0	5	6	4	0	2	3	5	1	2	3
GL	WV	12	0	1	5	1	0	0	0	0	0	0	3	2	2	105	0	3	0	0	0	0	0	1	0	0	0	0	0	0	5	3	0
	Sentinel	9	2	0	0	5	12	0	4	1	4	0	10	6	2	45	0	15	0	1	0	0	2	0	0	0	0	0	0	0	0	6	0
	SPOT	0	2	5	1	7	1	0	2	23	3	21	0	5	3	80	6	0	1	1	6	0	0	1	1	1	2	0	2	0	8	0
HA	WV	0	0	2	0	6	0	0	0	31	3	0	0	3	0	0	103	5	0	0	0	0	10	6	0	6	2	4	0	2	0	4
	Sentinel	0	2	3	0	0	0	3	12	16	0	35	1	4	2	0	20	1	3	1	1	8	9	2	7	3	0	10	24	4	6	10
	SPOT	7	2	1	0	5	4	2	3	1	0	1	0	0	0	0	45	2	0	1	3	1	3	0	2	2	1	0	3	0	9	0
KA	WV	3	0	0	1	3	8	0	1	2	5	1	1	2	10	0	0	109	0	8	1	2	7	2	7	0	0	0	0	0	1	0
	Sentinel	0	0	1	0	0	0	0	1	0	0	0	29	2	21	5	0	108	2	1	0	7	0	5	1	21	0	6	0	0	2	6
	SPOT	0	6	5	2	3	2	0	1	3	1	9	0	0	3	0	2	120	0	2	1	0	4	0	3	0	2	2	2	3	0	2
ZC	WV	2	9	2	1	0	3	2	0	6	66	0	8	4	3	2	3	1	50	0	0	1	0	3	2	0	0	0	0	7	11	0
	Sentinel	13	3	0	0	13	1	0	0	30	2	2	0	11	0	0	0	1	71	0	4	1	2	6	3	6	3	8	0	0	6	8
	SPOT	3	0	1	1	0	0	0	0	8	0	0	1	2	0	0	0	1	21	1	3	0	2	6	2	0	1	0	1	1	8	0

Table 4. (Continued).

PRED			AC	AD	AK	AM	BL	BR	CAf	CAu	CA	DN	DR	EC	ER	GB	GL	HA	KA	ZC	MA	Oea	PC	PV	RL	SH	SL	SM	SN	SP	TC	ZC	ZM
MA	WV		2	0	5	0	5	1	0	0	0	0	0	3	1	6	0	3	0	0	44	1	1	3	3	0	1	3	5	4	3	8	5
	Sentinel		0	0	0	0	0	1	1	4	0	12	1	3	1	10	3	4	0	0	99	0	1	0	1	5	0	0	2	6	0	0	2
	SPOT		0	0	5	0	3	6	4	2	10	1	1	0	1	2	3	2	3	0	30	2	0	3	1	0	2	1	0	0	6	1	0
OEa	WV		5	0	2	5	6	1	0	5	1	10	0	0	0	8	3	2	14	0	3	123	6	3	0	18	0	1	0	0	0	0	0
	Sentinel		0	5	0	0	0	0	0	0	30	0	0	2	8	2	0	1	2	4	0	87	1	5	0	0	0	0	8	6	1	0	0	6
	SPOT		10	2	4	0	3	1	0	1	3	3	6	1	0	0	0	1	0	0	3	35	0	3	5	0	0	3	3	2	6	10	3
PC	WV		0	0	1	1	5	0	8	0	12	0	0	10	3	9	1	0	11	0	5	16	98	6	0	0	1	0	0	0	0	25	0
	Sentinel		3	0	0	0	3	0	3	0	0	2	0	1	0	10	8	3	1	9	0	0	46	4	0	0	0	0	3	3	1	2	12	3
	SPOT		8	0	0	0	0	4	2	1	4	5	1	0	3	3	3	1	3	0	6	3	76	1	0	2	0	1	1	3	5	6	1
PV	WV		3	3	0	7	0	0	0	0	0	3	0	0	0	0	2	0	0	0	0	0	1	90	0	0	1	4	0	0	1	5	0
	Sentinel		12	12	36	0	0	0	3	0	2	0	0	1	0	12	1	0	0	1	0	0	0	54	0	0	0	3	7	5	4	6	7
	SPOT		0	1	3	0	8	3	0	2	2	2	2	1	0	4	5	4	4	0	2	0	0	80	1	2	25	22	3	1	2	0	3
RL	WV		0	7	0	1	5	9	6	4	2	0	0	13	0	1	7	1	3	3	1	1	0	0	50	0	0	0	2	0	0	0	2
	Sentinel		0	12	0	0	2	2	0	2	0	8	0	0	0	21	1	1	0	0	0	0	0	1	77	1	0	0	0	1	0	0	0
	SPOT		0	1	0	0	1	1	0	0	2	0	0	0	3	0	0	0	3	9	1	1	0	0	99	0	0	0	0	0	0	0	0
SH	WV		1	0	3	0	5	0	0	0	0	1	0	0	6	28	0	3	13	0	1	10	0	0	0	100	0	0	0	0	1	1	1	0
	Sentinel		0	1	0	0	3	0	0	0	1	0	0	0	0	2	2	1	0	5	1	0	1	2	2	70	0	5	5	13	1	2	5
	SPOT		2	1	0	1	0	5	0	1	3	12	2	0	0	0	2	1	0	0	10	2	1	2	2	82	3	2	2	1	0	0	2

Table 4. (Continued).

PRED		AC	AD	AK	AM	BL	BR	CAf	CAu	CA	DN	DR	EC	ER	GB	GL	HA	KA	ZC	MA	Oea	PC	PV	RL	SH	SL	SM	SN	SP	TC	ZC	ZM
SL	WV	4	0	2	5	3	7	0	3	5	5	0	4	0	2	1	1	0	0	1	3	3	2	1	0	99	15	2	3	1	0	2
	Sentinel	0	0	0	0	0	1	0	0	0	0	0	0	6	4	6	3	0	0	0	0	0	0	0	0	23	6	0	1	1	0	0
	SPOT	1	1	0	1	6	0	2	2	3	1	10	1	1	3	3	2	0	0	13	0	1	2	2	2	40	3	8	1	1	0	8
SM	WV	2	0	0	0	9	0	5	0	0	0	1	2	1	13	0	2	2	2	0	0	1	1	0	0	0	101	5	0	11	0	5
	Sentinel	0	2	33	0	2	0	1	0	0	20	0	1	0	1	0	0	1	0	0	4	1	0	0	2	1	55	7	7	0	0	7
	SPOT	0	6	3	2	23	2	0	1	0	0	6	0	0	4	1	1	2	2	1	0	4	5	2	1	1	60	1	0	1	0	1
SN	WV	4	2	0	1	2	0	10	1	1	5	0	5	4	6	0	3	0	2	0	4	6	0	1	1	0	16	80	0	0	3	80
	Sentinel	0	3	0	2	1	2	0	1	2	0	0	6	0	2	3	0	4	3	0	7	4	0	2	2	0	5	82	7	0	0	82
	SPOT	7	1	3	0	1	0	0	1	6	4	1	0	4	0	0	3	0	1	2	2	1	2	1	0	1	0	98	3	1	0	98
SP	WV	0	0	0	0	4	8	0	5	0	3	0	2	1	12	1	2	0	2	8	0	0	0	0	2	0	2	0	120	0	0	0
	Sentinel	3	2	0	2	2	3	8	1	1	12	3	6	1	0	8	0	0	3	1	3	2	0	2	10	36	5	5	55	0	0	5
	SPOT	4	2	6	0	9	0	0	0	2	2	5	0	3	4	4	2	4	1	0	1	0	5	1	2	3	4	2	92	0	3	2
TC	WV	8	0	0	3	1	1	0	0	10	9	1	14	0	3	1	3	0	2	1	0	12	0	1	0	0	3	2	7	67	0	2
	Sentinel	0	0	0	1	0	22	1	10	1	3	0	0	0	1	4	1	1	0	0	0	0	1	0	1	0	2	2	2	89	0	2
	SPOT	7	6	6	0	1	9	1	0	12	4	0	0	0	0	0	0	4	0	1	0	1	1	0	0	0	2	6	0	30	1	6
ZC	WV	0	0	5	3	8	2	0	0	4	3	21	0	0	33	0	3	0	7	0	1	5	10	0	3	2	1	6	0	0	90	6
	Sentinel	5	3	0	0	2	0	0	3	0	0	1	0	0	0	0	0	0	0	27	5	1	3	1	0	1	0	2	0	100	154	2
	SPOT	0	5	3	21	0	0	1	3	0	7	4	0	0	2	0	0	0	11	2	17	3	1	0	0	3	3	9	0	0	95	9

Table 4. (*Continued*).

	PRED	AC	AD	AK	AM	BL	BR	CAf	CAu	CA	DN	DR	EC	ER	GB	GL	HA	KA	ZC	MA	Oea	PC	PV	RL	SH	SL	SM	SN	SP	TC	ZC	ZM
																					REF											
WV	ZM	2	0	0	0	9	0	5	0	0	0	1	2	1	13	0	2	2	2	0	0	1	1	0	0	0	101	5	0	11	0	5
Sentinel		0	2	33	0	2	0	1	0	0	20	0	1	0	1	0	0	1	0	0	4	1	0	0	2	1	55	7	7	0	0	7
SPOT		0	6	3	2	23	2	0	1	0	0	6	0	0	4	1	1	2	2	1	0	4	5	2	1	1	60	1	0	1	0	1

Acknowledgments

Data Availability

The authors confirm that the data supporting the findings of this study are available within the article and Tables 3 and 4 in Appendix A and Appendix B.

References

1. M. S. M. Sosef et al., "Exploring the floristic diversity of tropical Africa," *BMC Biol.* **15**, 1–23 (2017).
2. E. Gyamfi-Ampadu, M. Gebreslasie, and A. Mendoza-Ponce, "Mapping natural forest cover using satellite imagery of Nkandla forest reserve, KwaZulu-Natal, South Africa," *Remote Sens. Appl. Soc. Environ.* **18**, 100302 (2020).
3. J. Ondier et al., "Influence of rainfall amount and livestock grazing on soil respiration in a moist Kenyan savannah," *Afr. J. Ecol.* **58**, 92–99 (2020).
4. E. E. Cleland et al., "Phenological tracking enables positive species responses to climate change," *Ecology* **93**(8), 1765–1771 (2012).
5. M. Hirschmugl et al., "Combined use of optical and synthetic aperture radar data for REDD + applications in Malawi," *Land* **7**, 116 (2018).
6. M. Sankaran, "Droughts and the ecological future of tropical savanna vegetation," *J. Ecol.* **107**, 1531–1549 (2019).
7. M. Lopes et al., "Combining optical and radar satellite image time series to map natural vegetation: savannas as an example," *Remote Sens. Ecol. Conserv.* **6**, 316–326 (2020).
8. C. P. Osborne et al., "Human impacts in African savannas are mediated by plant functional traits," *New Phytol.* **220**(1), 10–24 (2018).
9. Z. S. Venter, M. D. Cramer, and H. J. Hawkins, "Drivers of woody plant encroachment over Africa," *Nat. Commun.* **9**, 2272 (2018).
10. J. Barnetson, S. Phinn, and P. Scarth, "Mapping woody vegetation cover across Australia's arid rangelands: utilising a machine-learning classification and low-cost remotely piloted aircraft system," *Int. J. Appl. Earth Obs. Geoinf.* **83**(December 2018), 101909 (2019).
11. B. Zimbres et al., "Savanna vegetation structure in the Brazilian Cerrado allows for the accurate estimation of aboveground biomass using terrestrial laser scanning," *For. Ecol. Manage.* **458**(June 2019), 117798 (2020).
12. D. Rocchini et al., "Measuring β-diversity by remote sensing: a challenge for biodiversity monitoring," *Methods Ecol. Evol.* **9**, 1787–1798 (2018).
13. H. Xie, G. G. Wang, and M. Yu, "Ecosystem multifunctionality is highly related to the shelterbelt structure and plant species diversity in mixed shelterbelts of eastern China," *Glob. Ecol. Conserv.* **16**, e00470 (2018).
14. R. Avtar et al., "Potential application of remote sensing in monitoring ecosystem services of forests, mangroves and urban areas," *Geocarto Int.* **32**(8), 874–885 (2017).
15. M. P. Ferreira et al., "Mapping tree species in tropical seasonal semi-deciduous forests with hyperspectral and multispectral data," *Remote Sens. Environ.* **179**, 66–78 (2016).
16. T. Gao et al., "Timber production assessment of a plantation forest: an integrated framework with field-based inventory, multi-source remote sensing data and forest management history," *Int. J. Appl. Earth Obs. Geoinf.* **52**, 155–165 (2016).

17. J. G. Masek et al., "The role of remote sensing in process-scaling studies of managed forest ecosystems," *For. Ecol. Manage.* **355**, 109–123 (2015).
18. N. Clerici et al., "Estimating aboveground biomass and carbon stocks in periurban Andean secondary forests using very high resolution imagery," *Forests* **7**, 138 (2016).
19. T. Dube et al., "Remote sensing of invasive *Lantana camara* (Verbenaceae) in semiarid savanna rangeland ecosystems of South Africa," *Rangel. Ecol. Manag.* **73**, 411–419 (2020).
20. M. Kganyago et al., "Evaluating the capability of Landsat 8 OLI and SPOT 6 for discriminating invasive alien species in the African Savanna landscape," *Int. J. Appl. Earth Obs. Geoinf.* **67**(January), 10–19 (2018).
21. S. Khare, H. Latifi, and S. K. Ghosh, "Multi-scale assessment of invasive plant species diversity using Pléiades 1A, RapidEye and Landsat-8 data," *Geocarto Int.* **33**(7), 681–698 (2018).
22. G. Mandal and S. P. Joshi, "Eco-physiology and habitat invasibility of an invasive, tropical shrub (*Lantana camara*) in western Himalayan forests of India," *Forest Sci. Technol.* **11**, 182–196 (2015).
23. M. Niphadkar et al., "Comparing pixel and object-based approaches to map an understorey invasive shrub in tropical mixed forests," *Front. Plant Sci.* **8**, 892 (2017).
24. W. Ji and L. Wang, "Phenology-guided saltcedar (*Tamarix* spp.) mapping using Landsat TM images in western U.S.," *Remote Sens. Environ.* **173**, 29–38 (2016).
25. D. Rocchini et al., "Satellite remote sensing to monitor species diversity: potential and pitfalls," *Remote Sens. Ecol. Conserv.* **2**, 25–36 (2016).
26. T. Adole, J. Dash, and P. M. Atkinson, "A systematic review of vegetation phenology in Africa," *Ecol. Inf.* **34**, 117–128 (2016).
27. M. K. Heenkenda et al., "Mangrove species identification: comparing WorldView-2 with aerial photographs," *Remote Sens.* **6**(7), 6064–6088 (2014).
28. J. Zhou et al., "Comparison of GF2 and SPOT6 imagery on canopy cover estimating in northern subtropics forest in China," *Forests* **11**(4), 407 (2020).
29. M. Immitzer, C. Atzberger, and T. Koukal, "Tree species classification with random forest using very high spatial resolution 8-band worldView-2 satellite data," *Remote Sens.* **4**(9), 2661–2693 (2012).
30. H. Astola et al., "Comparison of Sentinel-2 and Landsat 8 imagery for forest variable prediction in boreal region," *Remote Sens. Environ.* **223**(January), 257–273 (2019).
31. M. Cross et al., "Classification of tropical forest tree species using meter-scale image data," *Remote Sens.* **11**(12), 1411 (2019).
32. G. Forkuor et al., "Landsat-8 vs. Sentinel-2: examining the added value of sentinel-2's red-edge bands to land-use and land-cover mapping in Burkina Faso," *GISci. Remote Sens.* **55**(3), 331–354 (2018).
33. C. Lin et al., "Classification of tree species in overstorey canopy of subtropical forest using QuickBird images," *PLoS One* **10**(5), 1–23 (2015).
34. D. Lewis, S. Phinn, and K. Pfitzner, "Pixel-based image classification to map vegetation communities using SPOT5 and Landsat5 thematic mapper data in a tropical savanna, northern Australia," *Can. J. Remote Sens.* **38**(5), 570–585 (2012).
35. E. Chuvieco and A. Huete, *Fundamentals of Satellite Remote Sensing*, CRS Press, Talyor and Francis Group (2009).
36. S. Ibrahim et al., "Estimating fractional cover of plant functional types in African savannah from harmonic analysis of MODIS time-series data," *Int. J. Remote Sens.* **39**, 2718–2745 (2018).
37. M. Karlson et al., "Assessing the potential of multi-seasonal WorldView-2 imagery for mapping West African agroforestry tree species," *Int. J. Appl. Earth Obs. Geoinf.* **50**, 80–88 (2016).
38. E. M. de O. Silveira et al., "Carbon-diversity hotspots and their owners in Brazilian southeastern Savanna, Atlantic Forest and semi-arid Woodland domains," *For. Ecol. Manage.* **452**(Aug.), 117575 (2019).
39. L. Zhu et al., "A review: remote sensing sensors," in *Multi-Purposeful Application of Geospatial Data*, B. R. Rustam et al., Ed., IntechOpen (2018).

40. A. C. Toniol et al., "Potential of hyperspectral metrics and classifiers for mapping Brazilian savannas in the rainy and dry seasons," *Remote Sens. Appl. Soc. Environ.* **8**, 20–29 (2017).

41. Z. H. Khwaja, W. Ahmad, and R. J. Williams, "An evaluation of alternative image classification techniques for the identification and mapping of tropical savanna landscape in Northern Australia," *Geocarto Int.* **18**(1), 33–44 (2003).

42. T. Gill et al., "A method for mapping Australian woody vegetation cover by linking continental-scale field data and long-term Landsat time series," *Int. J. Remote Sens.* **38**(3), 679–705 (2017).

43. Y. Wang et al., "Mapping tropical disturbed forests using multi-decadal 30 m optical satellite imagery," *Remote Sens. Environ.* **221**, 474–488 (2019).

44. N. B. Mishra, K. A. Crews, and G. S. Okin, "Relating spatial patterns of fractional land cover to savanna vegetation morphology using multi-scale remote sensing in the Central Kalahari," *Int. J. Remote Sens.* **35**, 2082–2104 (2014).

45. L. Mucina, L. W. Rutherford, and M. C. Powrie, *Biomes and Bioregions of Southern Africa*, South African National Biodiversity Institute (2006).

46. A. C. Kruger and M. P. Nxumalo, "Historical rainfall trends in South Africa: 1921–2015," *Water SA* **43**(2), 285–297 (2017).

47. M. G. Molezzi, K. A. A. Hein, and M. S. D. Manzi, "Mesoarchaean-Palaeoproterozoic crustal-scale tectonics of the central Witwatersrand basin: interpretation from 2D seismic data and 3D geological modelling," *Tectonophysics* **761**, 65–85 (2019).

48. S. E. Piovan, Ed., "Remote Sensing," in *Springer Geography*, Springer, Cham (2020).

49. www.digitalglobe.com.

50. https://scihub.copernicus.eu/dhus/.

51. P. S. Chavez, "Image-based atmospheric corrections: revisited and improved," *Photogramm. Eng. Remote Sens.* **62**, 1025–1036 (1996).

52. S. M. Adler-Golden et al., "Atmospheric correction for shortwave spectral imagery based on MODTRAN4," *Proc. SPIE* **3753**, 1–10 (1999).

53. P. Stych et al., "A comparison of worldview-2 and landsat 8 images for the classification of forests affected by bark beetle outbreaks using a support vector machine and a neural network: a case study in the sumava mountains," *Geosciences* **9**, 396 (2019).

54. C. Laben and B. Brower, "Process for enhancing the spatial resolution of multispectral imagery using pan-sharpening," United States Pat. 6 (2000).

55. D. Lu and Q. Weng, "A survey of image classification methods and techniques for improving classification performance," *Int. J. Remote Sens.* **28**, 823–870 (2007).

56. L. Ma et al., "Training set size, scale, and features in geographic object-based image analysis of very high resolution unmanned aerial vehicle imagery," *ISPRS J. Photogramm. Remote Sens.* **102**, 14–27 (2015).

57. K. W. Cassel, "Image processing and data analysis," in *Variational Methods with Applications in Science and Engineering*, C. Kevin, Ed., Cambridge University Press (2013).

58. M. Kuhn, "Building predictive models in R using the caret package," *J. Stat. Software* **28**, 1–26 (2008).

59. R Development Core Team, *R: A Language and Environment for Statistical Computing*, R Foundation for Statistical Computing (2020).

60. L. Breiman, "Bagging predictors," *Mach. Learn.* **24**, 123–140 (1996).

61. L. Breiman, "Random forests," *Mach. Learn.* **45**, 5–32 (2001).

62. C. Cortes and V. Vapnik, "Support-vector networks," *Mach. Learn.* **20**, 273–297 (1995).

63. A. E. Maxwell, T. A. Warner, and F. Fang, "Implementation of machine-learning classification in remote sensing: an applied review," *Int. J. Remote Sens.* **39**, 2784–2817 (2018).

64. A. Karatzoglou et al., "kernlab: an S4 package for kernel methods in R," *J. Stat. Software* **11**, 1–20 (2004).

65. K. Congalton and R. Green, *Assessing the Accuracy of Remotely Sensed Data. Principles and Practices*, 2nd ed., CRC Press, Boca Ratón (2009).

66. M. Story and R. G. Congalton, "Remote sensing brief accuracy assessment: a user's perspective," *Photogramm. Eng. Remote Sensing* **52**, 397–399 (1986).

67. Q. McNemar, "Note on the sampling error of the difference between correlated proportions or percentages," *Psychometrika* **12**(2), 153–157 (1947).

68. M. A. Cho, O. Malahlela, and A. Ramoelo, "Assessing the utility WorldView-2 imagery for tree species mapping in South African subtropical humid forest and the conservation implications: Dukuduku forest patch as case study," *Int. J. Appl. Earth Obs. Geoinf.* **38**, 349–357 (2015).

69. L. T. Waser et al., "Evaluating the potential of worldview-2 data to classify tree species and different levels of ash mortality," *Remote Sens.* **6**(5), 4515–4545 (2014).

70. P. Kayastha et al., "Effect of time window on satellite and ground-based data for estimating chlorophyll-a in reservoirs," *Remote Sens.* **14**(4), 846 (2022).

71. P. Macintyre, A. van Niekerk, and L. Mucina, "Efficacy of multi-season Sentinel-2 imagery for compositional vegetation classification," *Int. J. Appl. Earth Obs. Geoinf.* **85**, 101980 (2020).

72. Y. Xie, Z. Sha, and M. Yu, "Remote sensing imagery in vegetation mapping: a review," *J. Plant Ecol.* **1**, 9–23 (2008).

73. G. Mallinis et al., "A random forest modelling procedure for a multi-sensor assessment of tree species diversity," *Remote Sens.* **12**, 1210 (2020).

74. J. Odindi et al., "Comparison between WorldView-2 and SPOT-5 images in mapping the bracken fern using the random forest algorithm," *J. Appl. Remote Sens.* **8**, 083527 (2014).

75. I. Chrysafis et al., "Evaluation of single-date and multi-seasonal spatial and spectral information of Sentinel-2 imagery to assess growing stock volume of a Mediterranean forest," *Int. J. Appl. Earth Obs. Geoinf.* **77**, 1–14 (2019).

76. L. Eklundh, L. Harrie, and A. Kuusk, "Investigating relationships between landsat ETM+ sensor data and leaf area index in a boreal conifer forest," *Remote Sens. Environ.* **78**, 239–251 (2001).

77. A. Mellor et al., "The performance of random forests in an operational setting for large area sclerophyll forest classification," *Remote Sens.* **5**, 2838–2856 (2013).

78. R. S. Fletcher and K. N. Reddy, "Random forest and leaf multispectral reflectance data to differentiate three soybean varieties from two pigweeds," *Comput. Electron. Agric.* **128**, 199–206 (2016).

79. S. G. Tesfamichael et al., "Field spectroradiometer and simulated multispectral bands for discriminating invasive species from morphologically similar cohabitant plants," *GIScience Remote Sens.* **55**, 417–436 (2018).

80. J. Delegido et al., "Evaluation of sentinel-2 red-edge bands for empirical estimation of green LAI and chlorophyll content," *Sensors* **11**, 7063–7081 (2011).

Biographies of the authors are not available.